AL/HR-TR-1993-0189

VISUAL EVALUATION OF COMPUTER-GENERATED TEXTURES

George A. Geri
Don R. Lyon
Yehoshua Y. Zeevi

University of Dayton Research Institute
300 College Park Avenue
Dayton, OH 45469-0110

HUMAN RESOURCES DIRECTORATE
AIRCREW TRAINING RESEARCH DIVISION
6001 S. Power Road, Bldg 558
Mesa, AZ 85206-0904

January 1994

Final Technical Report for Period October 1990 - March 1993

Approved for public release; distribution is unlimited.

AIR FORCE MATERIEL COMMAND
BROOKS AIR FORCE BASE, TEXAS

ARMSTRONG LABORATORY

NOTICES

This technical report is published as received and has not been edited by the technical editing staff of the Armstrong Laboratory.

When Government drawings, specifications, or other data are used for any purpose other than in connection with a definitely Government-related procurement, the United States Government incurs no responsibility or any obligation whatsoever. The fact that the Government may have formulated or in any way supplied the said drawings, specifications, or other data, is not to be regarded by implication, or otherwise in any manner construed, as licensing the holder, or any other person or corporation; or as conveying any rights or permission to manufacture, use, or sell any patented invention that may in any way be related thereto.

The Office of Public Affairs has reviewed this report, and it is releasable to the National Technical Information Service, where it will be available to the general public, including foreign nationals.

This report has been reviewed and is approved for publication.

Elizabeth L. Martin
ELIZABETH L. MARTIN
Project Scientist

Dee H. Andrews
DEE H. ANDREWS, Technical Director
Aircrew Training Research Division

LYNN A. CARROLL, Colonel, USAF
Chief, Aircrew Training Research Division

REPORT DOCUMENTATION PAGE

Form Approved
OMB No. 0704-0188

1. AGENCY USE ONLY *(Leave blank)*	2. REPORT DATE	3. REPORT TYPE AND DATES COVERED
	January 1994	Final October 1990 - March 1993

4. TITLE AND SUBTITLE

Visual Evaluation of Computer-Generated Textures

5. FUNDING NUMBERS

C - F33615-90-C-0005
PE - 62205F
PR - 1123
TA - 03
WU - 85

6. AUTHOR(S)
George A. Geri
Don R. Lyon
Yehoshua Y. Zeevi

7. PERFORMING ORGANIZATION NAME(S) AND ADDRESS(ES)

University of Dayton Research Institute
300 College Park Avenue
Dayton, OH 45469-0110

8. PERFORMING ORGANIZATION REPORT NUMBER

9. SPONSORING / MONITORING AGENCY NAME(S) AND ADDRESS(ES)

Armstrong Laboratory (AFMC)
Human Resources Directorate
Aircrew Training Research Division
6001 S. Power Road, Bldg 558
Mesa, AZ 85206-0904

10. SPONSORING / MONITORING AGENCY REPORT NUMBER

AL/HR-TR-1993-0189

11. SUPPLEMENTARY NOTES

Armstrong Laboratory Technical Monitor: Dr. Elizabeth L. Martin, (602) 988-6561.

12a. DISTRIBUTION / AVAILABILITY STATEMENT

Approved for public release; distribution is unlimited.

12b. DISTRIBUTION CODE

13. ABSTRACT *(Maximum 200 words)*

Textures generated by superimposing sinusoidal luminance distributions can be used to simulate the natural terrain textures often used in flight simulator imagery. Since the visual system is spatially inhomogeneous with the periphery being generally less sensitive than the center of the visual field, simpler, more easily generated textures can potentially be used to simulate terrain that is farther from the operator's point of regard. The minimal number of component sinusoids required to generate textures that are visually acceptable in the visual periphery was estimated for the discrimination of complex suprathreshold textures. Specifically, similarity ratings were obtained to determine the effects of component orientation and component phase-bandwidth on the cortical magnification factor (CMF) associated with that discrimination. The textures were designed to be both specifically by a relatively small number of localized spectral components and sufficiently complex to approximate natural images. The number of component orientations was found to be a particularly important determinant of texture discrimination in that its effect on rated similarity was largely independent of the total number of components making up the texture. When the number of components was varied, a CMF of 2 was sufficient to equate the similarity ratings obtained at 0.75° and 20°. Under the same conditions, a CMF of 4 clearly overcorrected the data. The estimated CMF for texture discrimination is much smaller than that found for the discrimination of simple 2-D spatial frequency and suggests that either quantitatively different cortical mechanisms or different cortical areas are responsible for the two types of discrimination. When the phase-bandwidth of the component textures was varied, the data were not adequately corrected by the same CMF of 4 that overcorrected the component orientation data.

14. SUBJECT TERMS			15. NUMBER OF PAGES
Gabor functions	Phase	Vision models	46
Orientation	Textures		16. PRICE CODE
Perception	Vision		

17. SECURITY CLASSIFICATION OF REPORT	18. SECURITY CLASSIFICATION OF THIS PAGE	19. SECURITY CLASSIFICATION OF ABSTRACT	20. LIMITATION OF ABSTRACT
Unclassified	Unclassified	Unclassified	UL

CONTENTS

List of Figures

PREFACE

The present effort was conducted in support of the Armstrong Laboratory/Aircrew Training Research Division (AL/HRA) under Work Unit 1123-03-85, Flying Training Research Support, and by Air Force Contract F33615-90-C-0005 with the University of Dayton Research Institute. The laboratory contract monitor was Ms. Patricia A. Spears; task monitor was Dr. Byron J. Pierce.

The authors thank Chris Voltz for the image presentation and data collection software and Dr. David C. Hubbard for assistance with the statistical analysis. Portions of this work have been presented at annual meetings of the Association for Research in Vision and Ophthalmology (Geri, Lyon, & Zeevi, 1989, 1990).

VISUAL EVALUATION OF COMPUTER-GENERATED TEXTURES

SUMMARY

Many natural images, and in particular, natural textures, can be efficiently generated by adding together simple, sinusoidal luminance distributions. There are at least two advantages to this approach. First, the number of sinusoids required to generate a given texture is usually much less than the number of gray-levels required to specify a given texture on a point-by-point basis as is required, for instance, in a raster display system. Second, since the visual system is not equally sensitive at all points in the visual field, it is often possible to generate an image more efficiently if visual information is distributed in accordance with this sensitivity. Sinusoidal components can easily be modified so that they are spatially localized (the result is called a Gabor function), and as such they can be added together independently, and as required, at various locations in the image. In the present study, various complex textures were generated using Gabor functions of various spatial frequencies and orientations. These textures were then compared to textures generated using successively fewer Gabor functions in order to determine the minimal number of components necessary to generate a reduced texture that was visually similar to the original. We found that the number of orientational components was the most important determinant of texture discrimination in that its effect on the rated similarity of the textures was not dependent on the total number of components. We also found that in the case of properly constructed, wide-field imagery, between one-half and three-quarters of the components could be removed without significantly affecting the visual quality of the texture.

INTRODUCTION

Generating Images Using Spectral Components

Any periodic signal, including visual images, can be represented by an appropriately chosen series of weighted sinusoids. Natural images are often spatially periodic and hence are well represented in this way. Natural images are also often spatially redundant and can usually be represented by many fewer components than the number of elements required to generate the image point-by-point (cf. Geri, Zeevi & Porat, 1990). A spectral representation of images is also consistent with the postulated function of the visual system, which is believed to perform a Fourier-like analysis of visual stimuli (cf. Braddick, Campbell & Atkinson, 1978).

The concept of spectrally selective visual mechanisms was initially developed to explain threshold psychophysical data, and the most successful of the models incorporating this concept have confined themselves to predicting such data (Georgeson & Harris, 1984; Graham & Nachmias, 1971; Watson, 1982; Wilson & Bergen, 1979). There have, however, been numerous attempts to incorporate these mechanisms into models of suprathreshold discrimination (Cannon & Fullenkamp, 1988; Quick, 1974; Thomas, 1985; Watson, 1983), and even the discrimination of complex, real-world images (Caelli, 1982). Aside from the well-documented

problems associated with modeling nonlinear responses, there are two major difficulties in applying the visual mechanism concept to complex, suprathreshold imagery. The first problem is stimulus control. It is difficult to generate complex stimuli, which both approximate real-world imagery, and whose spatial frequency and orientation content are easily specified. It may be possible to reach a compromise, however, between the requirements for controlled stimuli on the one hand and realistic stimuli on the other by using stimuli that are composed of selected, discrete, spectral components. Stimuli of this kind can be well specified both spatially and spectrally and can be used to approximate natural images and other images with continuous power spectra (Field, 1987; Kronauer, Daugman & Zeevi, 1982; Porat & Zeevi, 1989). The second problem associated with applying the visual mechanism concept to complex, suprathreshold imagery is that it is often difficult to predict how component spatial frequency or orientation will manifest itself in complex stimuli. This has proven to be a problem even when relatively simple one-dimensional gratings are used (Badcock, 1984; Lawton, 1984). In the present study a higher-order perceptual response (similarity rating) was obtained to suprathreshold synthetic textures composed of multiple spectral components. While this approach makes it more difficult to relate the data to early visual mechanisms, it may reveal higher order aspects of the perception of visual texture which are not predictable from threshold data.

Assuming that the perception of 2-D spatial frequency (i.e., spatial frequency (SF) and orientation (OR)) is mediated by a relatively small number of overlapping mechanisms, it is conceivable that one of these mechanisms could be overstimulated in the sense that adding another component within the bandwidth of the mechanism could result in a relatively smaller change in the mechanism's output and hence an overall smaller perceptual difference in the stimulus. If this is true, then adding many components within a small frequency or orientation range may be an inefficient representation of the image in that a better selected distribution of components may give an adequate representation of the global properties of the image. If this is true, then at some point a density of sampling in spatial frequency or orientation will be reached at which the efficiency of stimulation of the mechanisms by each additional component will no longer be maximal.

One goal of the present study was to determine the minimum number of localized sinusoidal components necessary to preattentively represent a complex image composed of 64 components. This number was chosen as a compromise between the resolution attainable for a moderately sized image presented on available visual displays and the requirement that the textures reflect at least some of the complexities inherent in natural scenes (Porat & Zeevi, 1989).

The Cortical Magnification Factor (CMF)

It is well established that the visual field is nonhomogeneously mapped onto the visual cortex such that more cortical area is devoted to processing stimuli that are nearer to the center of the visual field (Daniel & Whitteridge, 1961; Talbot & Marshall, 1941; Van Essen, Newsome

& Maunsell, 1984). This fact, along with the observation that performance on most visual tasks declines as a function of retinal eccentricity (cf., Raninen & Rovamo, 1986), Rovamo & Virsu, 1979) has led to the concept of a cortical magnification factor (CMF). It is presumed that the level of performance on a visual task is related to the cortical area devoted to that task, and thus, that performance at different retinal eccentricities can be equated by scaling the size of the more peripheral stimulus by the CMF.

Human foveal sensitivity requires that very high resolution displays be used to present imagery at the point of fixation. Since it is beyond current technology to generate and display such high resolution over the entire visual field, some form of variable-resolution technique must be used to efficiently simulate the visual environment (Zeevi, Porat & Geri, 1990). The CMF is thus particularly relevant to visual simulation in that it specifies the required distribution of visual information as a function of distance from the fixation point. In the present study we have estimated a CMF for the discrimination of complex textures similar in appearance to those used in many flight simulators (Schachter, 1980, 1983). The textures used here have the added advantage that they are composed of spectral components and hence can be readily incorporated in full gray-scale imagery using image generation techniques that are both mathematically complete and computationally efficient (Porat & Zeevi, 1988; Zeevi & Gertner, 1992).

The CMF associated with certain positional judgments such as vernier acuity (Klein & Levi, 1987; Levi, Klein & Aitsebaomo, 1985) and phase discrimination (Bennett & Banks, 1991; Hess & Pointer, 1987) is typically greater than would be expected based on the anatomical and neurophysiological data. This has led to the suggestion that the visual periphery is inherently insensitive to positional relationships due either to its limited sampling capability (Snyder, 1982) or to a deficit in neural processing (Levi & Klein, 1985; Virsu, Näsänen & Osmoviita, 1987). In order to further assess the visual response to position-related characteristics of complex stimuli, we have also estimated a CMF for the discrimination of changes in structural coherence associated with increases in the phase-bandwidth of multicomponent textures.

Component Orientation and Phase-Bandwidth

Among the most salient features of psychophysically defined visual mechanisms is their selectivity for spatial frequency and orientation (Campbell & Robson, 1968; Carpenter & Blakemore, 1973; Graham & Nachmias, 1971). These features are also conspicuous in the response properties of individual neurons at many levels in the visual system (Enroth-Cugell & Robson, 1966; Gattass, Sousa & Covey, 1985), as well as in the topography of the visual cortex (Hubel & Wiesel, 1962, 1968). Daugman (1980, 1984) has emphasized the canonical relationship between spatial frequency and orientation and the importance of considering both of these variables in assessing the inherently two-dimensional response properties of visual receptive fields. These principles are now generally accepted, and hence in most recent studies, no preference is accorded to either spatial frequency or orientation. However, these studies usually involve threshold responses to relatively simple stimuli. It has proven more difficult to apply simple neural models to the discrimination of more complex stimuli (Caelli, 1982; Klein

& Tyler, 1986; Malik & Perona, 1990), and such models certainly cannot be expected to quantitatively predict the data obtained from higher order, or more cognitive, visual tasks. It might therefore be worthwhile in this context to determine the degree to which higher order perceptual responses to complex stimuli reflect, at least qualitatively, the properties of putative two-dimensional spatial frequency mechanisms.

The ability to discriminate both spatial frequency and orientation is known to decrease with retinal eccentricity, and this decrease can usually be compensated by applying an appropriate CMF (Johnston, 1987; Nothdurft, 1985; Rovamo, Virsu & Näsänen, 1978; Scobey, 1982). However, stimulus characteristics that might appear related to spatial frequency and orientation are often processed differently and may even result in different estimates of the CMF. For instance, Nothdurft (1985) found that the minimum line orientation that could be discriminated was generally smaller than the orientation difference required to discriminate adjacent textures. Also, the CMFs estimated by Scobey (1982) for a line orientation task were less than one-half those estimated by Paradiso and Carney (1988). Thus it is difficult to generalize estimated CMFs even from one relatively simple visual discrimination to another. Given that more than one component process may be involved in discriminating complex stimuli, and given that more complex discriminations may be mediated by higher (and progressively more integrative) cortical areas, it might be expected that the discrimination of simple and complex stimuli would involve different CMFs (cf. Gattass *et al.*,1985; Levi *et al.*, 1985).

In the present study the number of component orientations in a set of synthetic textures was varied in order to determine whether the perceptual salience of this parameter, which has been noted in previous studies (cf., Beck, 1982; Julesz, 1981), is also evident in the discrimination of full gray-scale textures. Measurements were obtained both near the fovea and in the peripheral visual field in order to estimate a CMF for this discrimination.

Modeling Complex Texture Discrimination

Texture perception research has typically used so-called microtexture patterns composed of fields of small, relatively simple elements and only a few gray levels (e.g., Beck, 1982; Julesz, 1981). It is clearly difficult to generalize from such stimuli to natural images, which typically comprise multiple gray-scales and often display a characteristic power spectrum (Field, 1987). It is likewise difficult to generalize the results of many of the current models of texture perception (cf. Clark & Bovik, 1989; Fogel & Sagi, 1989; Graham, Beck, & Sutter, 1992) that are based on mechanisms inferred from neurophysiological work on visual receptive fields. These studies have used relatively simple stimuli and sets of feature analyzers that match the textures whose discrimination is being modeled. While many of the results have justified this approach, texture segregation models must ultimately predict the discrimination of more complex, natural textures (Caelli, 1982). One appropriate set of stimuli for testing these models could be generated by adding together localized spectral components such as those used in the present study. Such stimuli have been shown to approximate natural textures (Porat & Zeevi,

1989), and they would be conveniently analyzable in terms of a physiologically plausible set of feature analyzers.

It has been recognized (cf. Badcock, 1984) that suprathreshold stimuli consisting of even a few sinusoidal components can manifest perceptually salient, local luminance "features" that cannot be predicted solely from the response of simple mechanisms to those components. Although the present state of development of texture models is not sufficient to predict the perceptual response to arbitrary suprathreshold stimuli, there may be aspects of the perception of such stimuli that are consistent with the general tenets of current models and which may constrain or help to delineate the proper form of future models. For instance, early research (Beck, 1966, 1982; Julesz, 1981) found that the orientation of the pattern elements making up a texture was an important determinant of texture segregation, and this is consistent with more recent quantitative models based on oriented detectors (Clark & Bovik, 1989; Fogel & Sagi, 1989; Graham, Beck, & Sutter, 1992). We have applied the texture discrimination model of Sutter, Beck, and Graham (1989) to the multicomponent texture stimuli used in the present study. This model was chosen because it incorporates many of the features of the other models and it has been developed in the context of experimental tasks and texture stimuli most similar to those used in the present study. The results are relevant both to assessing the generality of the model and to establishing additional criteria for evaluating this and other texture segregation models.

METHODS

Observers. Three observers, two females and one male (GG), participated in the present series of experiments. Observers LK and SP were in their mid-twenties, were unaware of the purpose of the study, and were compensated for their participation. Observer GG was 38 years old and was one of the authors. All observers had normal uncorrected vision.

Apparatus. Stimulus generation, data collection, and data analysis were under the control of an IBM PC-AT and a PCVision video board (Imaging Technology Inc., see Fig. 1). Stimuli were presented on Conrac monitors (Model 7241C19) using only the green channel (P22 phosphor). For the central (0.75 deg) condition, the two textures (see below) making up each stimulus were presented on the same monitor and were viewed at a distance of 3 m after reflection by two front-surface mirrors. The stimuli were presented in the upper half of the monitor display which provided a total illuminated area of 3.8 by 7.6 deg. The fixation point was a small black dot which was placed directly on the monitor screen. For the peripheral (20 deg) condition, the same pairs of textures (suitably scaled, see below) were presented on two separate monitors that were viewed directly from a distance of 1.5 m. A large cardboard screen was used to provide a homogeneous surface between and around the monitors. Two holes were cut in the screen such that only the left texture of the stimulus pair on the left monitor and the right texture of the stimulus pair on the right monitor were visible. The resulting visual

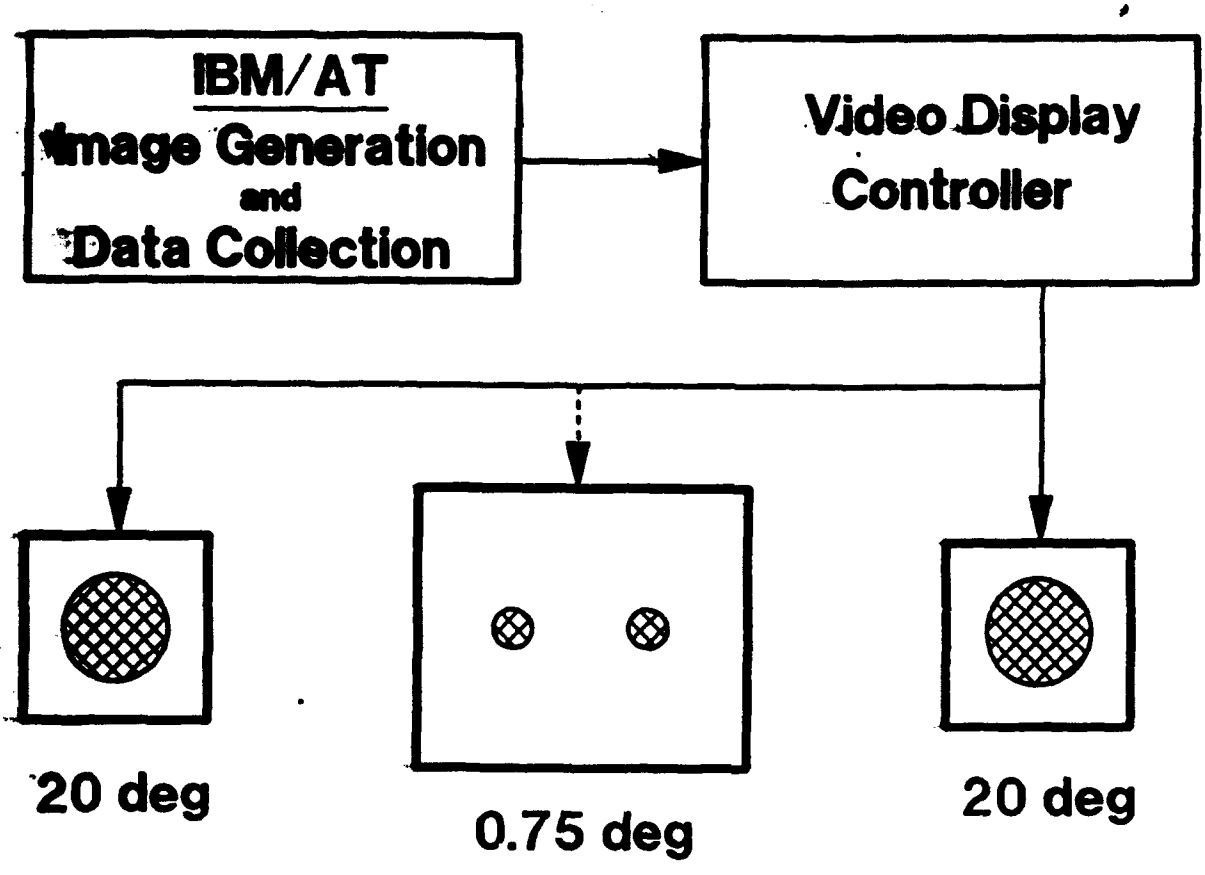

Figure 1
A Schematic Diagram of the Apparatus Used in the Present Study
Pairs of stimuli were presented either 0.75° or 20° on either side of the fixation point. Although both pairs are shown here, only one pair of stimuli was presented in a given experimental session. Sizes and distances are described in the text and are not shown to scale.

impression was that the two halves of the monitor display used in the central condition had been separated along the horizontal meridian. A green LED mounted in the cardboard screen midway between the two monitors served as a fixation point.

The stimulus display monitors were calibrated using a Spectra Spotmeter photometer (Photo Research). The function relating image pixel value to monitor luminance was linearized using a look-up table constructed in accordance with the measured response characteristics of the monitors. The mean luminance of the texture stimuli was 14 fL, and the experimental room was otherwise dark. The observers were provided with a chin and head rest and were asked to enter their rating response on a computer keyboard.

Stimuli. For both the orientation-components and phase-bandwidth stimulus sets, two-dimensional textures (see Fig. 2a) were generated off-line using a program which added together between 12 and 64 Gabor functions each with a luminance distribution, L(x,y) of the form:

$$L(x,y) = \exp\{-\pi[[\frac{x}{D}]^2 + [\frac{y}{D}]^2]\} \cdot \cos(\omega_x x + \phi_x + \omega_y y + \phi_y), \quad (1)$$

where D is the effective width ($\pm 1\sigma$) of the Gaussian window, ω_x and ω_y are the spatial frequency projections in the horizontal and vertical directions, respectively, and ϕ_x and ϕ_y are the associated phase shifts. The spatial frequencies referred to in this report correspond to

$$\sqrt{\omega_x^2 + \omega_y^2}\,. \quad (2)$$

The component spatial frequencies for each texture were distributed logarithmically between 1 and 12 cycles/deg (see Fig. 2b). This was accomplished by first generating a series of numbers, A_i, from 0 to 1, according to the formula, $A_i = (i-1)/(N-1)$, where N is the number of spatial frequencies in the set, and i is an integer between 1 and N. The spatial frequencies for the set were then determined by raising 12 to the A_ith power for each of the N A_i's. The results of this procedure for N=8 are shown in Table 1. Various numbers (M) of orientations were associated with each of the spatial frequencies determined as described above. Specifically, the orientations were linearly spaced between 0 deg and 180-(180/M) deg (see Fig. 2b).

For the stimuli used to investigate the effects of number of component orientations, each of the Gabor components making up a particular texture had the same effective width but no two had both the same number of spatial frequencies (#SFs) and the same number of orientations (#ORs). Each component also had a unique phase. The level of phase quantization among components depended on the number of components (n) in the texture. For an n-component texture, the levels of phase quantization used corresponded to the values of 2π*m/n radians where m is an integer between 1 and n. In order to minimize the effects of local luminance

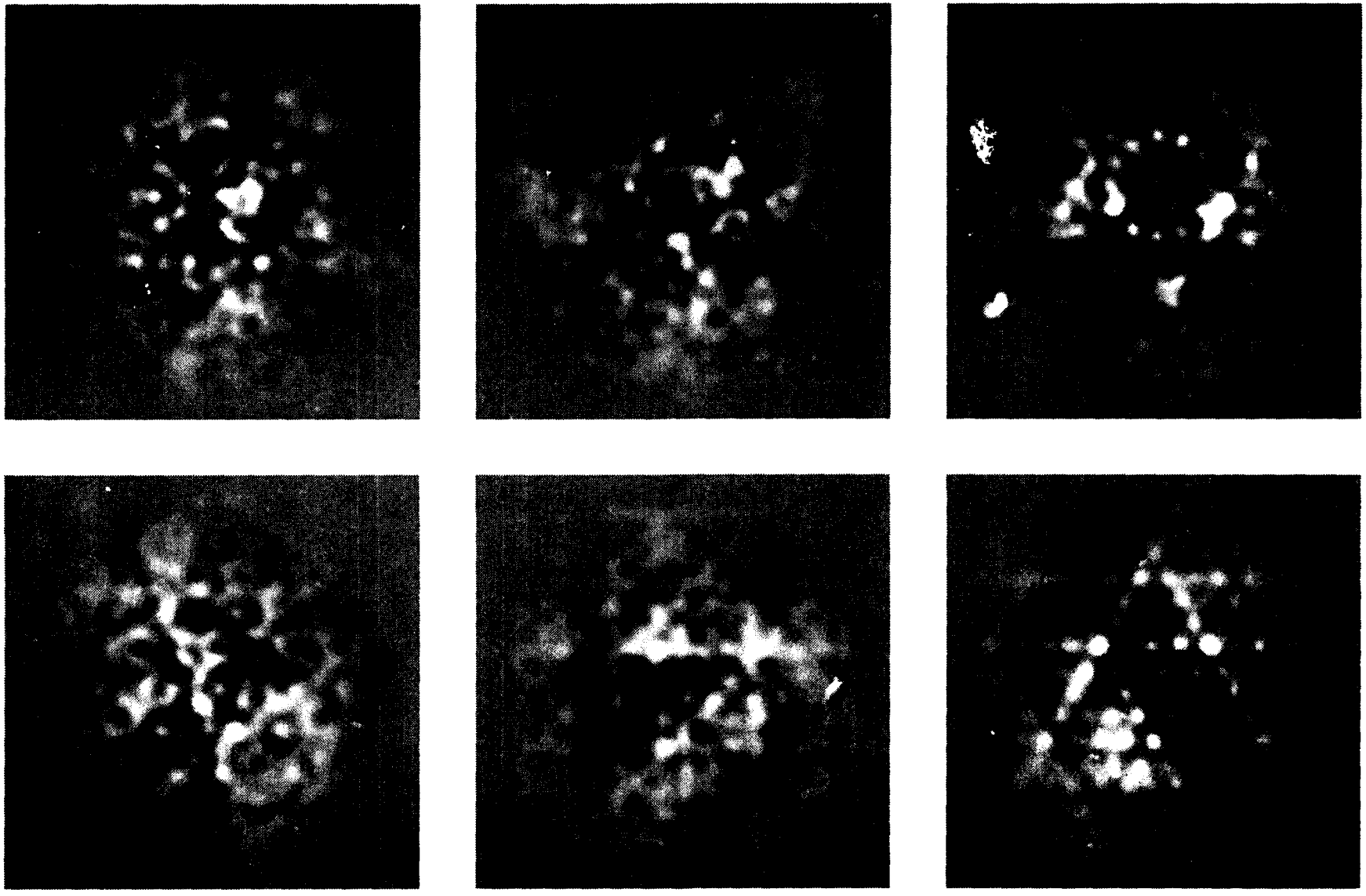

Figure 2a
A Typical Texture Set Used in the Orientation Portion of the Present Study
The textures in this set are composed of eight spatial frequencies at each of 8, 7, 6, 5, 4 or 3 orientations.

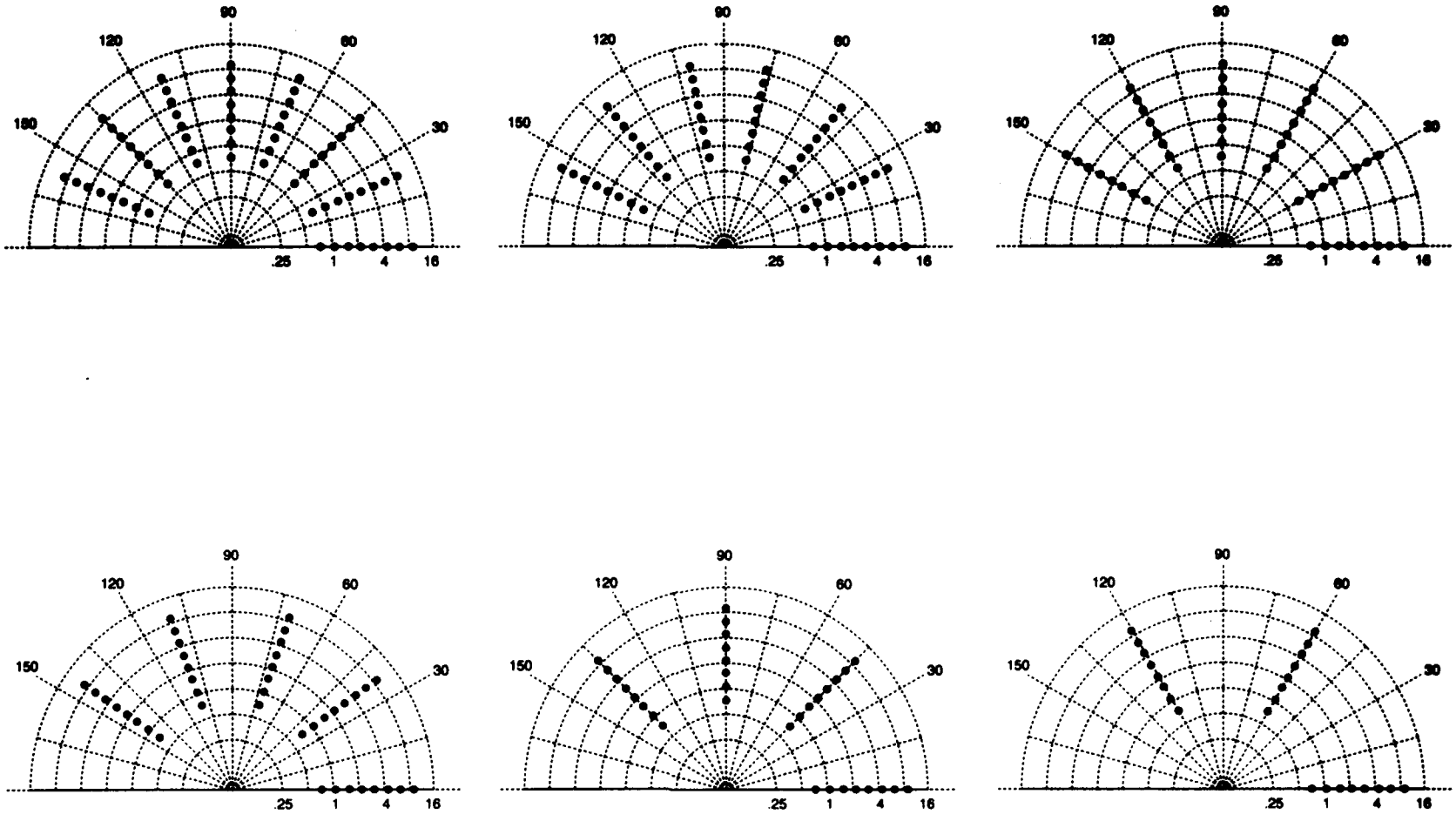

Figure 2b

The Component Distribution for Each Member of the Texture Set Shown in Figure 2a. The component phases for all textures were randomized. The texture at the upper right (8SFs/8ORs) is one of the textures that was used as a standard stimulus on each trial. The other three standard stimuli were obtained by randomly redistributing the component phases of the 8SF/8OR texture.

Table 1. Computation of the Spatial Frequency Levels (in cycles/Gaussian halfwidth) Used in a Gabor Texture Containing N=8 Spatial Frequencies

i	A_i	ω
1	0.000	1
2	0.143	1.43
3	0.286	2.04
4	0.429	2.9
5	0.571	4.13
6	0.714	5.9
7	0.857	8.41
8	1.000	12

variations on the similarity judgments, four different phase stimuli were generated for each #SFs-#ORs combination. The four stimuli were generated by randomly reassigning each of the phases, obtained as described above, to the various components of the original stimulus.

For the stimuli used to investigate the effects of phase-bandwidth, textures were generated by adding together either 24 or 64 Gabor functions. Four groups of textures were produced, using the following combinations of #SFs and #ORs, respectively: 4 and 16, 4 and 6, 8 and 8, and 8 and 3. Once again, the phase of each Gabor component relative to the center of the texture was randomly determined. In this portion of the study, the main independent variable was phase-bandwidth, defined as the width of the region (in phase space) over which the phases of the component Gabor functions were distributed. Shown in Figure 3 is the phase distribution of a hypothetical 24-component stimulus set. In order to avoid extensive areas of luminance saturation especially near the center of the resultant image, one-half of the components was distributed about phase=0 radians and the other half was distributed about phase=π radians. The phase bandwidths tested were determined by the parameter r (see Fig. 3) which was set equal to 0 (i.e., all components at the same phase), 13/3, 13/4, 13/5, and 13/6. An example of a phase bandwidth stimulus set (corresponding to 8SFs/8ORs) is shown in Figure 4a. The bandwidths corresponding to this and all other sets used in the present study correspond to $2\pi/r$ and hence equal 0, $6\pi/13$, $8\pi/13$, $10\pi/13$, and $12\pi/13$ radians. The textures shown in Figure 4a were obtained by distributing components in phase space in the manner shown in Figure 4b.

The stimuli presented at 0.75° eccentricity were 0.75° in diameter (at $\pm 1\sigma$) and the stimuli presented at 20° eccentricity were either 1.5° or 3.0° in diameter (i.e., CMFs of 2 and

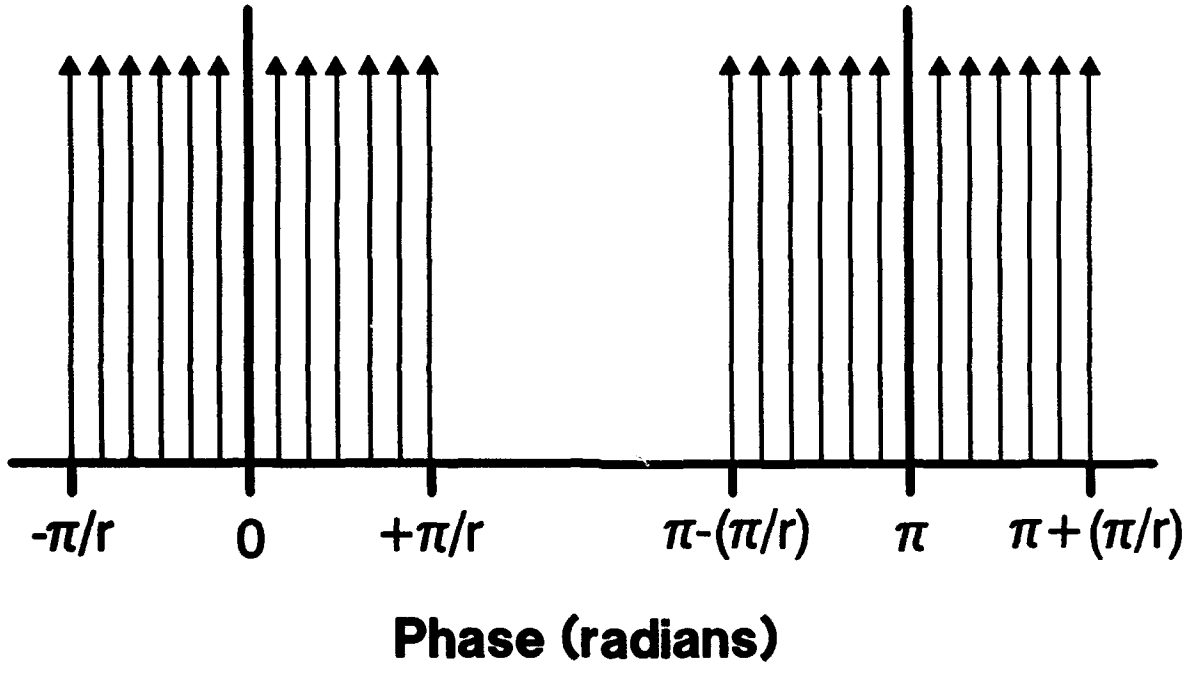

Figure 3
The Distribution in Phase Space of the Components
of a Hypothetical 24-Component Texture

One-half of the components were distributed around zero phase and one-half about π phase in order to avoid loss of texture structure due to the luminance saturation that occurred near the center of the image where the Gaussian envelope peaked for all components. The parameter, r, determines the phase-bandwidth and is inversely proportional to it.

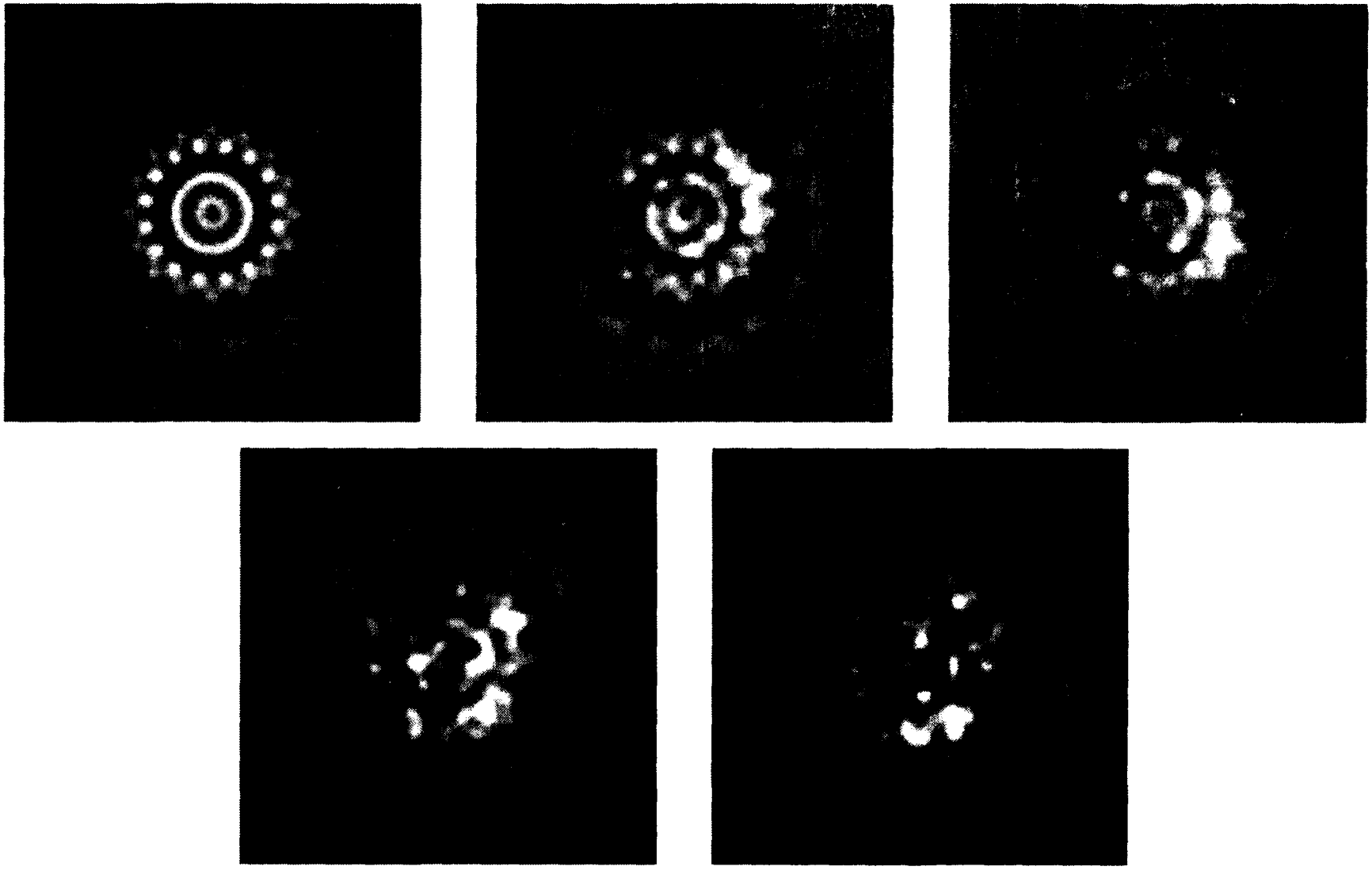

Figure 4a
A Typical Texture Set Used in the Phase-Bandwidth Portion of the Present Study
A wider distribution in phase space is asociates with a greater spatial
disruption of the original texture pattern shown at the upper left.

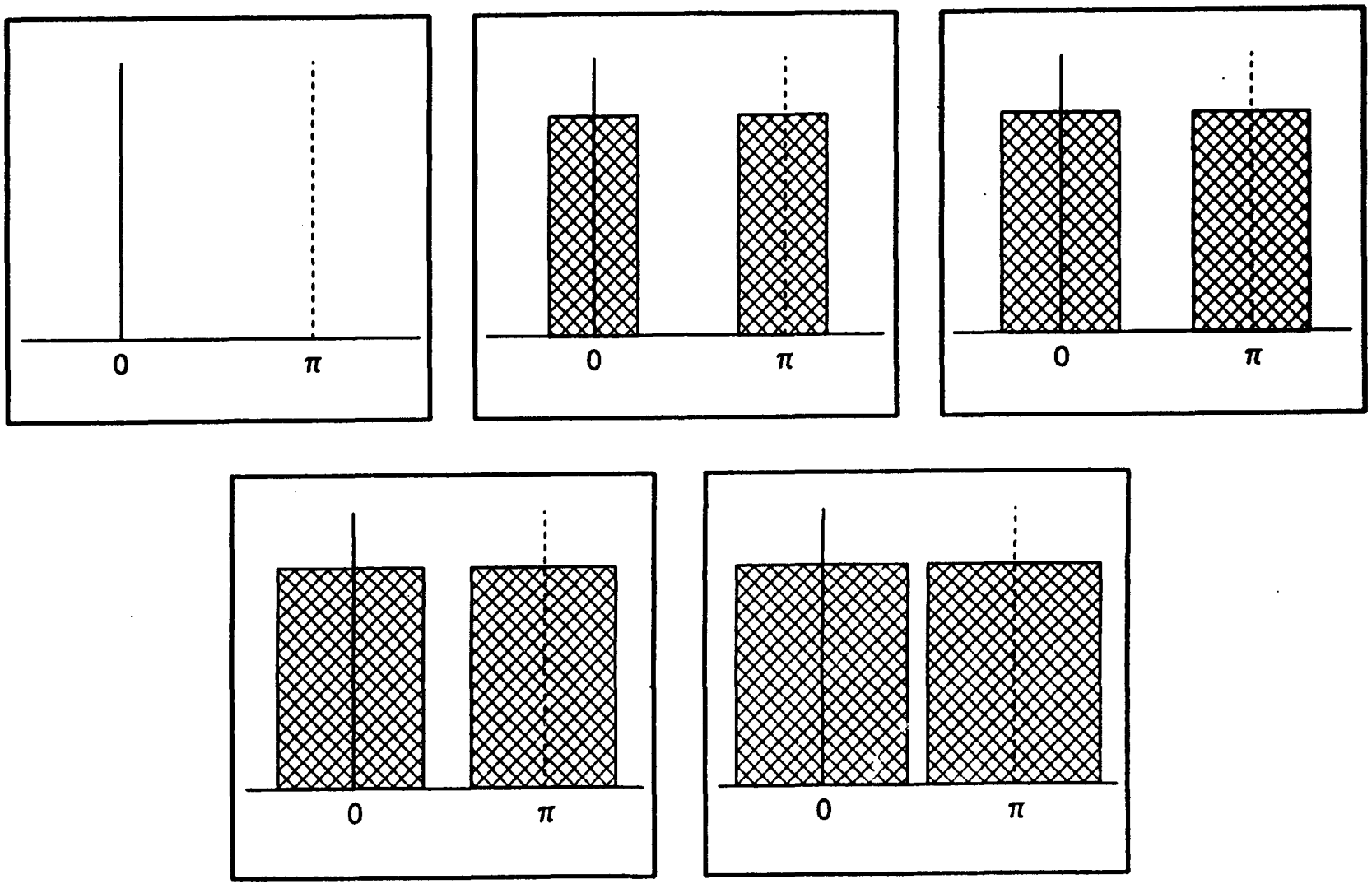

Figure 4b
The Phase Bandwidth Associated with Each Member of the Texture Set of Figure 4a. Each of the textures shown is composed of 64 components (8SFs and 8ORs) evenly distributed in phase space over the areas shown in the graphs.

4). The CMF of 4 was the largest we could test given the size of the display monitor and our desire to minimize observer accommodation by maintaining a viewing distance of at least 1.5m.

When modulating a sinusoidal luminance distribution by a Gaussian, a shift in the mean luminance results whenever the sinusoid is not antisymmetrical about the center of the Gaussian (i.e., for all sinusoids except a sine wave with phase equal to an integer multiple of π radians). Since the textured patterns extended over only a portion of the display, there would be a mismatch in the mean luminances of the textures and the background if image contrast were maximized using the most straightforward luminance scaling procedure of assigning the minimum (maximum) display luminance value to the minimum (maximum) pixel values. Therefore, to assure that the mean luminance of the pattern would match that of the background, the luminance range of each multicomponent texture was scaled as follows. Either the maximum pixel value in the texture was set equal to the maximum luminance (i.e., twice the mean luminance), or the minimum value was set equal to the minimum luminance, depending on whether the minimum (most negative) or maximum (most positive) pixel value was farther from zero. Although the Gaussian envelope theoretically extends to infinity in all directions, in practice it was limited to $\pm 2\sigma$ with all pixels beyond this limit set equal to the mean luminance.

Procedure. The observers first adapted for about five minutes to the ambient illumination in the experimental room. The last minute of adaptation was spent viewing a homogeneous field corresponding to the mean luminance of the stimulus textures to be presented. The observers initiated the session using their keyboard, and the first texture pair was presented for 167 ms. The observer then rated the similarity of the members of the pair by pressing the appropriate numeric key on the keyboard. The next pair was presented 2 s after the observer's response, and this cycle continued for the remainder of the session. In the component-orientation portion of the study, 18 combinations of #SFs and #ORs were tested in each session. Each of the 4 phase-versions corresponding to each #SF-#OR category was paired with each of the 4 phase-versions in the #SFs=8/#ORs=8 category--the latter thus serving as stimuli. Each of the resulting pairs was presented 8 times (4 with one of the standards on the right and 4 with it on the left) in each experimental session, resulting in a total of 18 x 4 x 8 = 576 trials randomized with respect to all variables mentioned above. The three combinations of eccentricity and test stimulus diameter (referred to here as the eccentricity-size factor) were tested in a different order for each observer. The testing procedures were similar in the phase-bandwidth portion of the study, except that there was a single standard stimulus corresponding to each of the four stimulus sets described earlier. The phase-bandwidth of the standard stimuli was zero indicating that half of the components had a phase of zero and half had a phase of π radians.

For both the component-orientations and phase-bandwidth portions of the study, the observers were asked to rate, on a scale from 1 (most dissimilar) to 7 (most similar), the perceived similarity of the two textures making up each stimulus. At least two practice sessions were run to acquaint the observers with the full range of possible differences between the pairs of textures. As noted above, in the component-orientation portion of the study, there were four phase versions of each of the standard and test stimuli. Similarity ratings were therefore obtained between each phase version of each stimulus and each phase version of the standard

(i.e., the stimulus for which #SFs = 8 and #ORs = 8). Thus, a high similarity rating does not necessarily mean perceptual equivalence since the baseline for each observer's ratings is the perceived difference not among physically identical stimuli but rather among stimuli that differed in the distribution of phase among each of their components.

Data Analysis. For the component-orientations portion of the study, data from the 0.75°/0.75° condition were compared with data from each of the other two conditions (20°/1.5° and 20°/3.0°) in two separate analyses of variance (ANOVAs). Each of the ANOVAs included three factors (eccentricity size, #SFs, and #ORs), and were performed using a randomized block design with observers as the block. Only some levels of the #ORs factor were included (i.e., those that were assessed at more than one level of the #SFs factor.) Even so, there was a small number of missing cells because these two factors were not completely crossed. All observer interactions were pooled into a single error term which was used to test the significance of all main effects and interactions.

For the phase-bandwidth portion of the study, data from the 0.75°/0.75° condition were again compared with data from each of the other two conditions (20°/1.5° and 20°/3.0°) in separate ANOVAs. Each of these ANOVAs included four, completely crossed factors (phase bandwidth, eccentricity size, number of components, and observer). Each of the data sets analyzed in the two ANOVAs described above was further analyzed by four additional ANOVAs, one for each of the two levels of the number-of-components factor for each of the two observers.

RESULTS

Since our initial concern was the relationship between rated similarity and number of components, our initial analysis was performed on these two variables. Examples of these data from one observer and one eccentricity-size condition are shown in Figure 5. The data show that the general shape of the rating functions is the same for each number of spatial frequencies, and that there appears to be a systematic shift along the horizontal axis as a function of the number of spatial frequencies in the stimulus texture. This suggested that number-of-orientations was the appropriate variable on which to perform subsequent analyses.

Number of Orientations

Shown in Figure 6 are mean similarity ratings, plotted as a function of the number of orientations (#ORs) in the test stimulus, for all three observers and all three eccentricity-size conditions. The three sets of points within each of the nine panels were obtained using test stimuli containing either 4, 6, or 8 spatial frequencies. As can be seen from the figure, there is considerable overlap among the three sets of points, indicating that the number of spatial frequencies (#SFs), and hence the total number of components in the texture stimulus has relatively little effect on perceived similarity. This observation is supported by a nonsignificant #SFs main effect and a nonsignificant #SFs x #ORs interaction in each of the two ANOVAs.

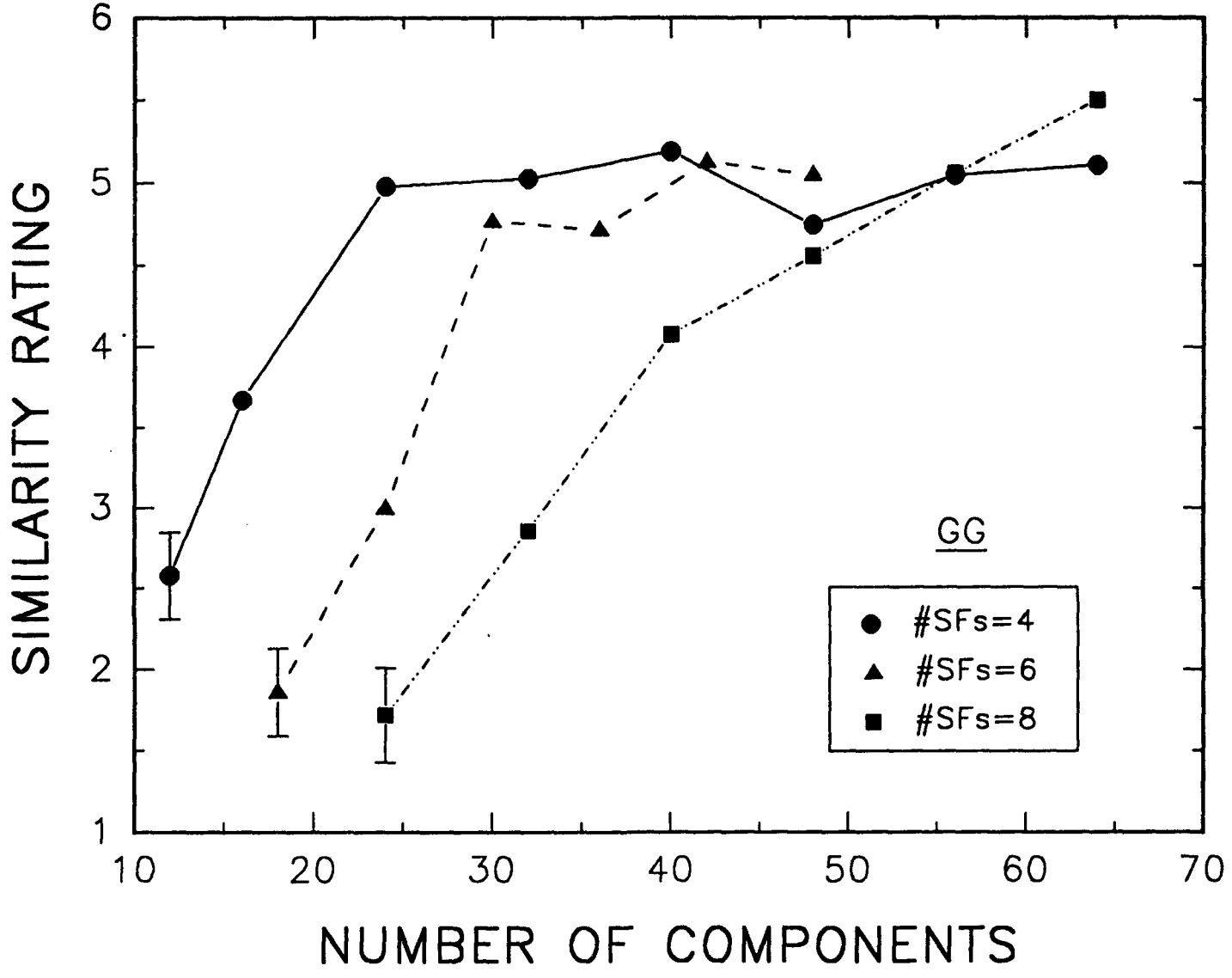

Figure 5

Similarity Ratings as a Function of the Number of Components in Three Sets of Textures Composed of Either 8, 6, or 4 Spatial Frequencies

The data for all numbers of spatial frequencies have a similar form suggesting that they might be accounted for by a single function if similarity rating were plotted against number of orientations (see Figure 6). The error bars represent mean 95% confidence limits for the data points of each curve.

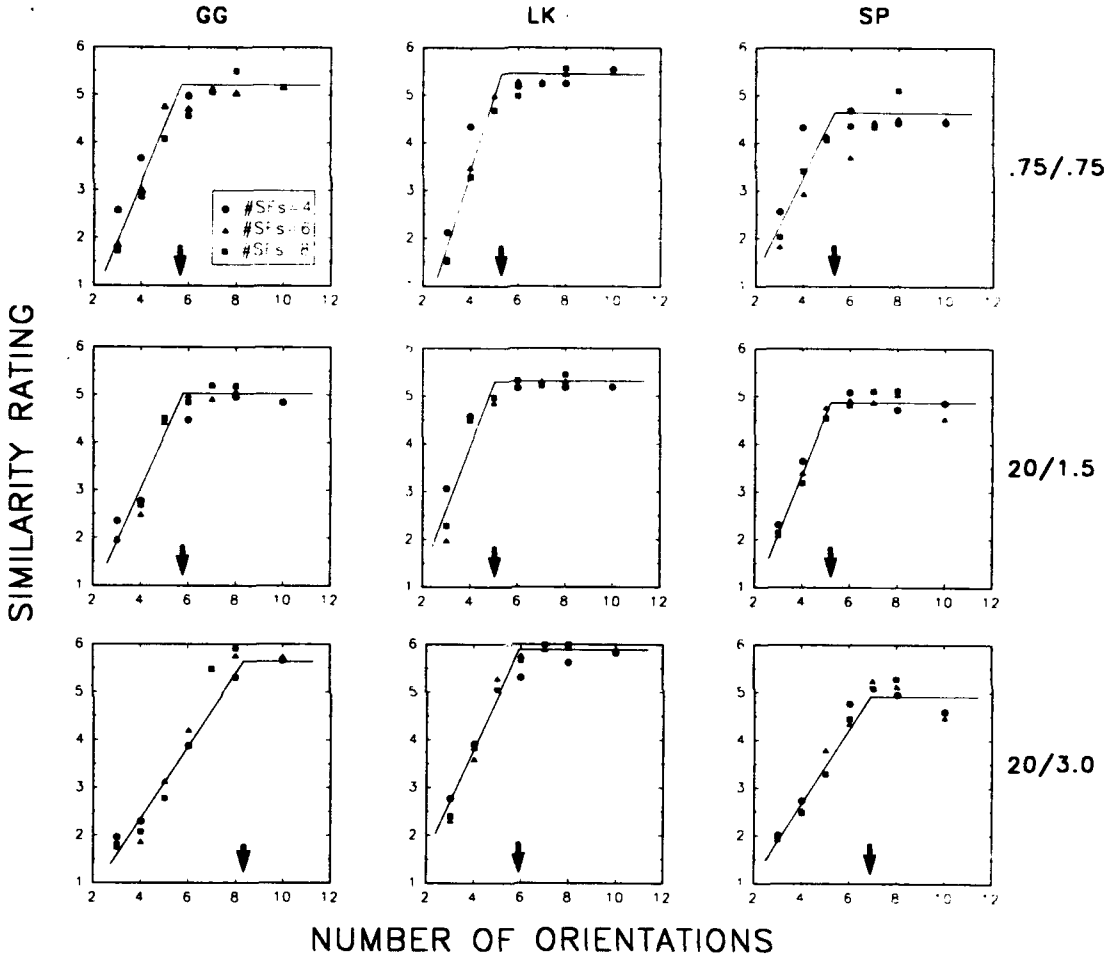

Figure 6
Similarity Ratings for Each of the Three Observers as a Function of the Number of Orientations (#ORs) Making Up the Stimulus Textures
Each panel shows a data set replotted from one similar to that of Figure 5. The top panel for each observer shows data obtained for a texture pair (i.e., 0.75° standard and test) presented at 0.75° on either side of the fixation point. The middle panels show the data obtained for textures composed of the same components but doubled in size to 1.5° (a CMF of 2) and presented at 20° eccentricity. The bottom panels show the data obtained using 3.0° textures (a CMF of 4) again presented at 20°.

As is evident from the data of Figure 6, rated similarity initially increased as the #ORs in the test stimuli were increased, and then remained approximately constant as the #ORs approached (and exceeded) the #ORs (i.e., 8) in the standard stimuli. This observation is reflected in the significant #ORs main effect in both the ANOVA comparing the 0.75°/0.75° and 20°/1.5° conditions ($F_{6,67}=142$, $p<10^{-4}$) and the ANOVA comparing the 0.75°/0.75° and 20°/3.0° conditions ($F_{6,69}=138$, $p<10^{-4}$). In order to estimate the critical #ORs (i.e., the #ORs at which rated similarity no longer changes as the #ORs are increased), we have fitted two straight lines to the data in each panel of Figure 5 using a least-squares criterion. A horizontal line was fitted to the rating data obtained for 8 and 10 orientations, and a second straight line was fitted to the rating data obtained for 3, 4, and 5 orientations. The intersection of the two regression lines in each panel was used to estimate the critical #ORs--that is, the #ORs above which the test textures were perceived to be as similar to the standard textures as the various phase versions of the standard textures were to themselves. Estimates of the critical #ORs are indicated by the arrows placed along the horizontal axis in each of the panels of Figure 6.

For all observers, the #ORs at asymptote are approximately the same for the 0.75°/0.75° and 20°/1.5° conditions, which is consistent with the fact that the eccentricity size x #ORs interaction did not even approach significance in the ANOVA comparing these two conditions ($F_{6,67}=0.26$, $p=0.95$). Further, there was no main effect of eccentricity size. Thus, doubling the size of the peripheral texture stimuli was sufficient to produce ratings similar to those obtained for the smaller stimuli near the fovea. In contrast, the #ORs at asymptote for the 20°/3.0° condition are greater than for the 0.75°/0.75° condition, and this is reflected in the significant eccentricity size x #ORs interaction in the ANOVA comparing these conditions ($F_{6,69}=4.72$, $p<.0004$).

For purposes of comparison, similarity rating was also plotted as a function of the number of spatial frequencies (#SFs) in the test stimulus, for two of the original three observers and all three eccentricity-size conditions. The results are shown in Figure 7 where it can be seen that the plot for #ORs=4 is generally flatter than the analogous plots for #ORs=6 and 8. This reinforces the conclusion, drawn from the same data plotted in Figure 6, that 6 and 8 orientations are generally at or above the estimated critical #ORs while 4 is below it.

Phase-Bandwidth

Mean similarity ratings as a function of phase-bandwidth, obtained from observers GG and LK, are shown in Figures 8a and 8b, respectively. The four panels in each figure correspond to the four combinations of #SFs/#ORs tested. For the two ANOVAs (one comparing the foveal condition with each of the peripheral conditions), all main effects and interactions were significant ($p<10^{-4}$) except for the observer x bandwidth and number-of-components x eccentricity-size interactions. Both ANOVAs indicated a significant decrease in rated similarity as phase-bandwidth was increased ($F_{4,7634}=1087$, $p<10^{-4}$; $F_{4,7000}=893$, $p<10^{-4}$). The decrease was greater for the foveal condition than for either of the peripheral conditions, as indicated by significant bandwidth x eccentricity-size interactions ($F_{4,7634}=74.2$, $p<10^{-4}$;

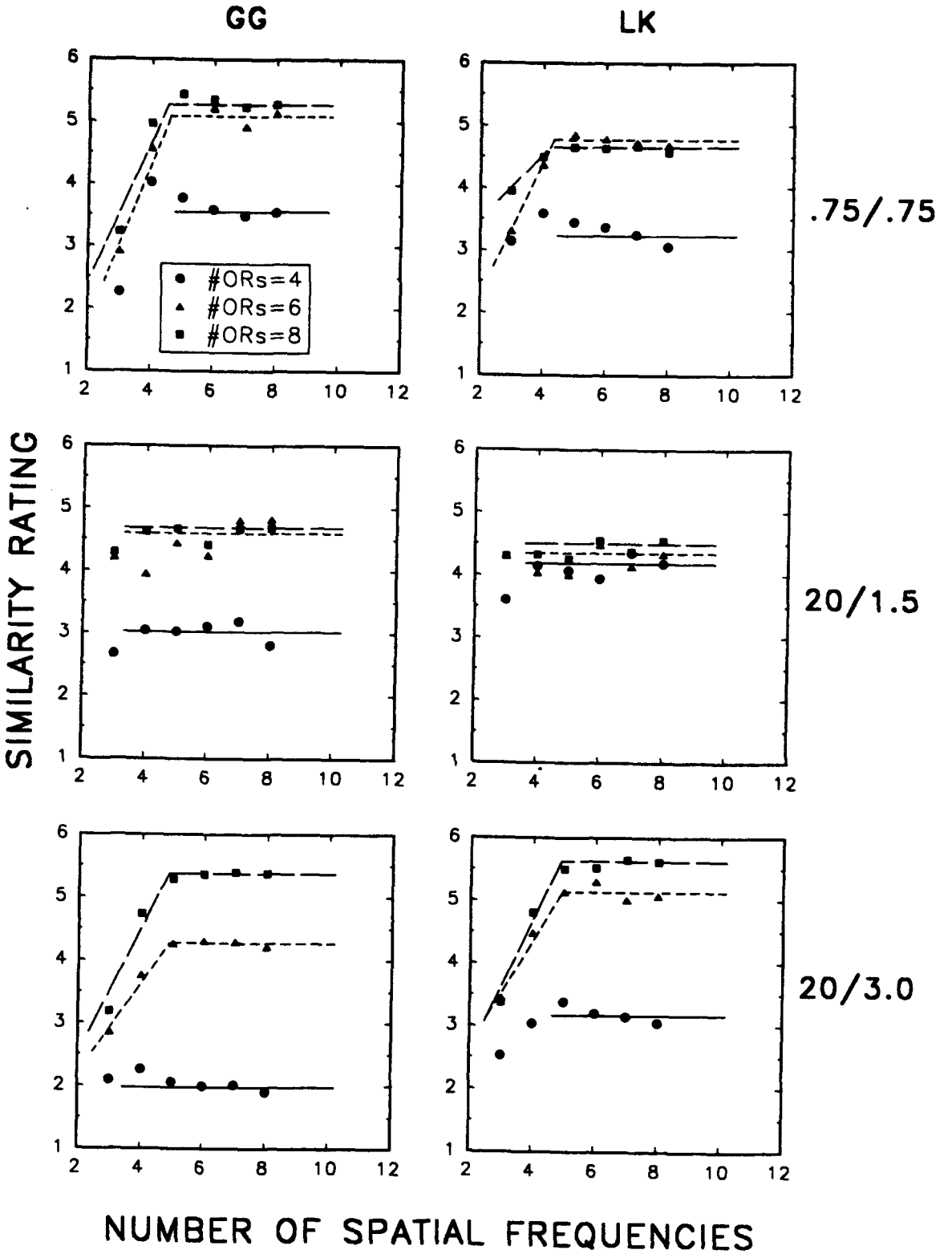

Figure 7
Similarity Ratings for Two Observers as a Function of the
Number of Spatial Frequencies (#SFs) Making Up the Stimulus Textures
The top panel for each observer shows data obtained for a texture pair (i.e., a 0.75° standard and a o.75° test) presented at 0.75° on either side of the fixation point. The middle panels show the data obtained for textures composed of the same components but doubled in size 1.5° (a CMF of 2) and presented at 20° eccentricity. The bottom panels show the data obtained using 3.0° textures (a CMF of 4) again presented at 20°.

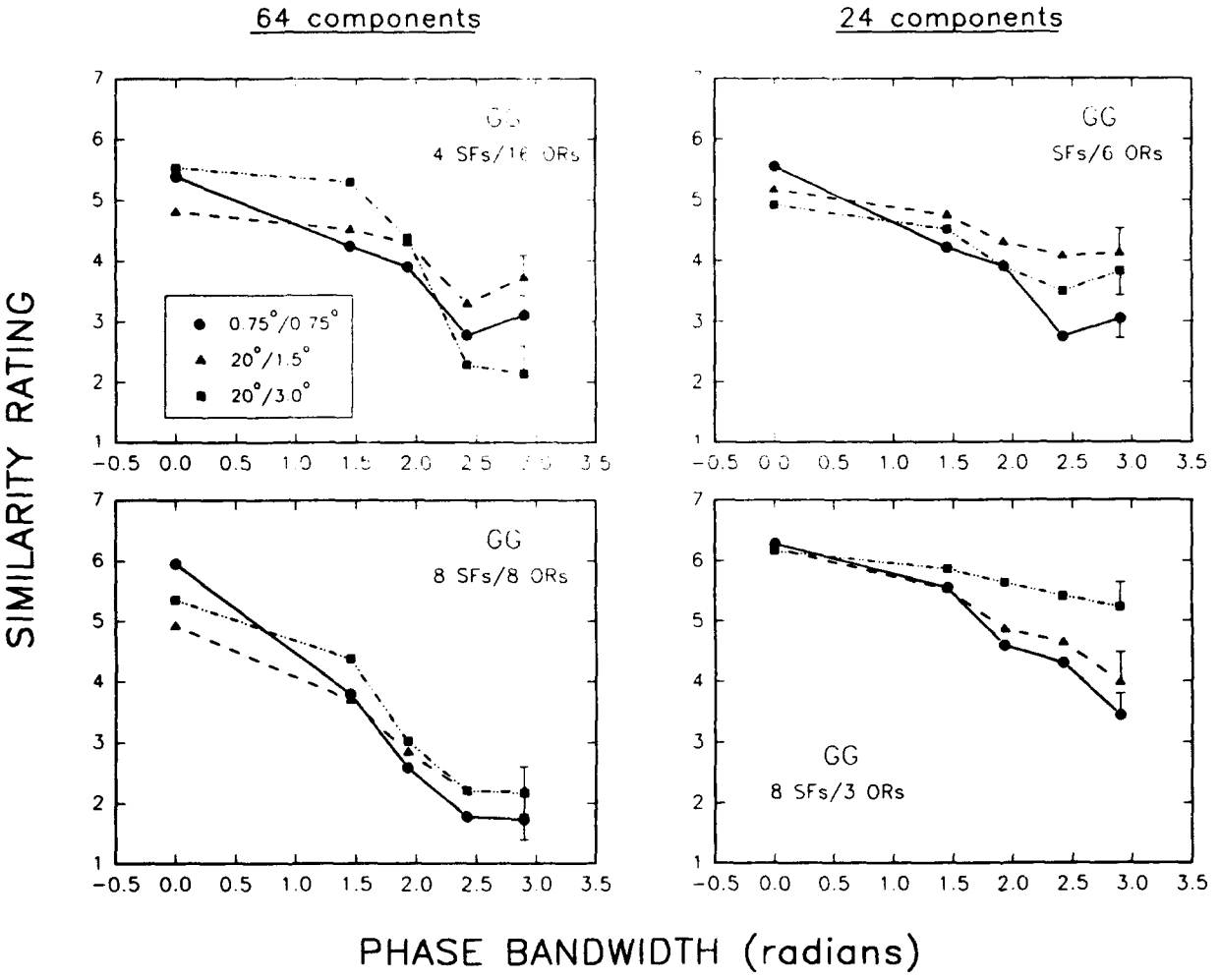

Figure 8a

Similarity Ratings as a Function of Phase-Bandwidth Data for Observer GG

For 0.75° stimuli presented at 0.75° eccentricity (filled circles) and for either 1.5° or 3.0° stimuli (representing CMFs of 2 and 4, respectively) presented at 20° eccentricity. Data for observer GG obtained using either 64 (left two panels) or 24 total components and an orientation density (#ORs/ #components) of either one-quarter (upper two panels) or one-eighth.

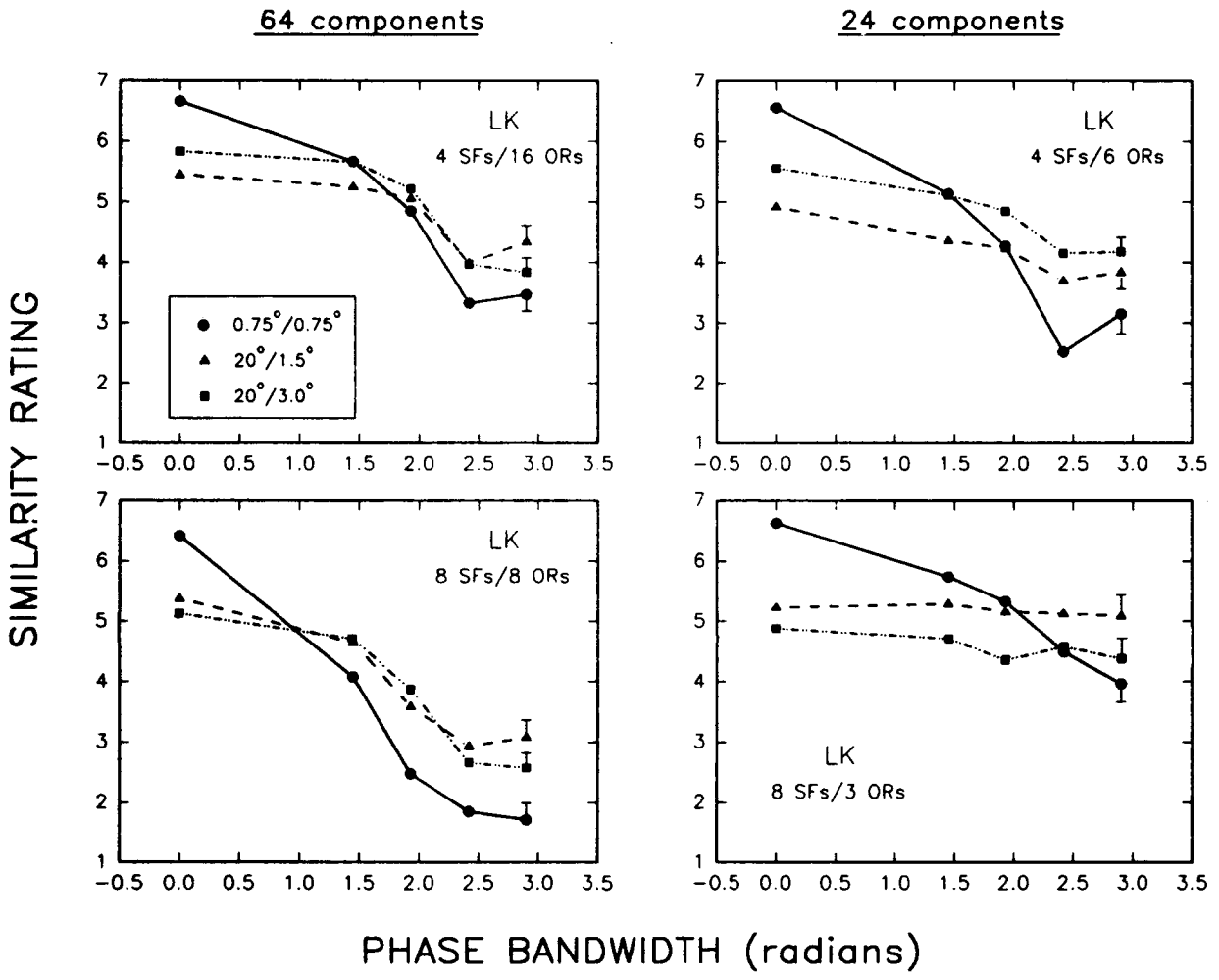

Figure 8b

Similarity Ratings as a Function of Phase-Bandwidth Data for Observer LK

For 0.75° stimuli presented at 0.75° eccentricity (filled circles) and for either 1.5° or 3.0° stimuli (representing CMFs of 2 and 4, respectively) presented at 20° eccentricity. Data for observer LK obtained using either 64 (left two panels) or 24 total components and an orientation density (#ORs/ #components) of either one-quarter (upper two panels) or one-eighth.

$F_{4,7000}=115$, $p<10^{-4}$). The significant bandwidth x eccentricity-size x number-of-components interactions ($F_{4,7634}=25.2$, $p<10^{-4}$; $F_{4,7000}=3.49$, $p<0.008$) further indicate that the difference between the size of the bandwidth effects in the foveal and peripheral conditions varied with number-of-components. Of the four additional ANOVAs, performed in order to determine which level (24 or 64) of the number-of-components factor resulted in the larger bandwidth x eccentricity-size interaction, the relevant F-ratios of three (all except number-of-components = 24 for observer GG) showed that the interaction was larger for the smaller number of components.

DISCUSSION

Complex Imagery from Spectral Components

Human spatial vision is presumed to be mediated by overlapping mechanisms, each with a bandwidth of one to two octaves (cf. Graham, 1989). This general view has been derived from threshold data, and even for those data it may not predict responses to complex stimuli composed of as few as two or three superimposed sinusoids (Badcock, 1984; Lawton, 1984). Although the present state of development of the mechanism doctrine may not be sufficient to predict the perceptual response to complex, suprathreshold stimuli, there may be aspects of the perception of such stimuli which are consistent with the predictions of that doctrine (or which may at least constrain or help to delineate the situations where it may effectively be applied). One of the questions that motivated the present research was whether there was, for a complex image, a minimum number of components which would produce an adequate perceptual representation of it. The answer to this question depends on the criteria chosen both to define image complexity and to determine what is an adequate perceptual representation. In the context of the postulated mechanisms of spatial vision, a complex stimulus could contain as few as two sinusoidal components, whereas thousands of such components are required to represent the complexity encountered in natural images. Once an appropriate level of image complexity is chosen, the most direct way to determine the minimum number of components needed to adequately represent the image is to first reconstruct it using successively more components and then to compare these partial reconstructions to the original.

Given a fixed number of components with which to construct an image, how is the best way to distribute them? In general it might be supposed that components which are very similar in spatial frequency and/or orientation would interact so that the perceptual difference between two such components and one within the same region of the visual field would be smaller than it would be if the two components were separated more widely in SF and/or OR. For both of the present studies, our major concern is with what may be considered emergent properties of texture discrimination--specifically, the perceptual similarity of gratings composed of different numbers of components, and the perceptual disruption of image structure as phase-bandwidth is increased. Although it may not be possible at present to establish how such emergent properties are related to the overall pattern of activity in the presumed set of mechanisms, it is

certainly useful to determine whether they change in a predictable way with known changes in mechanism properties which occur, for instance, across the visual field.

Salience of Component Orientation

The data of Figure 5 show, as might be expected, that rated similarity increases as the number of components making up the test texture approaches the number of components in the standard texture. More surprising perhaps is that the rate of increase in perceived similarity is largely independent of the #SFs in the texture series. This is true despite the fact that the three texture series, which produced the individual functions of Figure 5, are easily distinguishable, and that all textures were rated relative to the same (phase) set of 8OR/8SF standard textures. The similarities in the form of the functions of Figure 5 become more obvious when rated similarity is plotted as a function of the number of orientations in the test texture. Data plotted in this form are shown in the upper row of Figure 6 for each of the three observers at a retinal eccentricity of 0.75°. Plotting the data in this way is justified by the ANOVA results described earlier, and clearly shows that the #ORs in the test texture are the primary determinant of perceived similarity.

The orientation of pattern elements is known to be an important determinant of both threshold and suprathreshold form perception. For instance, differences in the orientation of texture micropatterns can underlie both perceptual grouping (Beck, 1966) and preattentive texture segregation (Beck, 1982; Julesz, 1981; Nothdurft, 1985). The visual salience of pattern orientation is reflected also in the orientation columns in the visual cortex (Carpenter & Blakemore, 1973; Hubel & Wiesel, 1962). The orientation columns are in turn one manifestation of presumed visual channels (Hubel & Wiesel, 1968) that have a two-dimensional spatial (and spectral) structure with an inherent orientation. The data of Figure 6 suggest, however, that orientation and spatial frequency may not be perceptually equivalent. Specifically, whereas the data indicate that component orientation is a particularly salient determinant of texture appearance, the fact that ratings are lower for textures composed of fewer orientations but not for those composed of fewer spatial frequencies suggests that the same perceptual importance is not attached to component spatial frequency.

The above-described salience of component orientation is a higher-order perceptual property that is not readily predictable from the responses of the visual processes that are presumed to underlie threshold spatial vision. In general, modeling higher-order perception using these visual processes has been successful only for selected stimuli (e.g., Bergen & Landy, 1991; Clark & Bovik, 1989; Graham, Beck & Sutter, 1992; Turner, 1986). Caelli and Bevan (1983) obtained similarity ratings for the comparison of broadband-filtered stochastic textures with their orientation-filtered counterparts. For the spatial frequency range below 8 c/deg, which is similar to that used in the present study, their results were consistent with threshold data obtained using simpler stimuli. The spectral components making up the stimuli used in the present study (see Fig. 2) correspond in some ways to visual weighting functions (cf. Jones & Palmer, 1987) and represent an extension of the stimulus set used by Caelli and Bevan in that

orientation is explicitly defined in the spatial domain. Thus, it might be expected that even similarity ratings obtained for the present stimuli would reflect in some aspect the response properties of basic visual mechanisms. Some evidence that this is the case can be seen in the critical #ORs estimated from the intersection of the functions fitted to the data in the upper row of Figure 6. The critical #ORs are between 5 and 7 and are therefore consistent with threshold data, which suggest that there are 5-8 orientation channels with bandwidths of 15-30 deg (Dannemiller & Ver Hoeve, 1990; Daugman, 1984; Phillips and Wilson, 1984). Correlations of this sort have also been noted in the context of other suprathreshold texture discriminations (cf., Caelli, 1982; Richards & Polit, 1974). Thus, we conclude from the data of Figure 6 that complex, suprathreshold textures can be generated which are *preattentively* indistinguishable from textures containing many more components, provided that the former contain at least 5-7 orientations. These results may also be applicable to real-world imagery in that spectral textures similar to those used here can be chosen to visually match many natural textures (Porat & Zeevi, 1989) as well as textures derived from other continuous spectra (Kronauer, Daugman & Zeevi, 1982).

CMF for Suprathreshold Textures

Orientation-Components Stimuli. A CMF for the discrimination of suprathreshold, full gray-scale textures has not to our knowledge been previously estimated. The importance of component orientation in determining the similarity rating of these textures suggests, however, that their CMF may correspond to those obtained for other orientation-related, preattentive discriminations. Estimates for the latter are available from several sources. Scobey (1982) found that the discrimination of line orientation could be equated at the fovea and the retinal periphery if line length was scaled in accordance with the size of cortical receptive fields as reported by Hubel and Wiesel (1974). He determined that a CMF of about 3.3 was sufficient to equate discrimination at 0° and 10° eccentricity. Virsu *et al.* (1987) have noted that Hubel and Wiesel's data are consistent with the psychophysical data of Rovamo and Virsu (1979) and hence would predict that a CMF of six would equate Scobey's data at 0.75° and 20° eccentricity. Also, Paradiso and Carney (1988) concluded that their orientation discrimination data could be adequately scaled using the CMF estimated by Levi *et al.* (1985) from the data of Dow, Snyder, Vautin and Bauer (1981). Those data give a relative CMF of about 14 between 0.75° and 20° eccentricity. Nothdurft (1985) measured both orientation sensitivity and the discrimination of textures composed of lines whose orientation differed. Although he concluded that the two tasks are mediated by functionally distinct mechanisms, his data indicate that performance on both tasks can be equated at 0.75° and 20° eccentricity if the more peripheral stimuli are scaled by a factor of about 7. Virsu *et al.* (1987) determined the orientation threshold for a two-dot vernier discrimination, and again, the data were found to be consistent with the CMFs estimated by Rovamo and Virsu (1979). Finally, Geri and Lyon (1991) estimated a CMF of 6 for shape adaptation to closed contour stimuli whose orientation was varied systematically. Thus, the available data on orientation-related discrimination predict a CMF of at least 6 between 0.75° and 20° eccentricity.

The data in the third row of Figure 6 were obtained at 20° eccentricity using a CMF of 4 relative to that used to obtain the data in the first row of that figure (corresponding to 0.75° eccentricity). Even this relatively low CMF resulted in an overcorrection of the data, in that both rated similarity and the critical #ORs (indicated by the arrows in Fig. 6) were significantly higher at 20° eccentricity. In an attempt to better estimate a CMF for our textures, the data in the second row of Figure 6 were then obtained (also at 20° eccentricity) using a CMF of 2. This CMF appears to adequately reproduce the ratings obtained at 0.75° eccentricity in that both the maximum rating and the derived critical #ORs are now very similar. Thus, the CMF estimated here for the similarity rating of complex textures is significantly lower than those estimated for simpler orientation-related discriminations.

The available data suggest that the visual cortex is organized hierarchically with higher levels performing successively more complex visual analyses (cf., van Essen & Maunsell '83). Complex, spatially separated, suprathreshold textures and a similarity rating task were used in the present study and thus the data of Figure 6 probably reflect a relatively high level of visual processing (cf. Lamme, Van Dijk & Spekreijse, 1992). Gattass *et al.* (1985) have summarized neurophysiological estimates, which indicate that the CMF is generally lower for higher visual-cortical levels. Although there appear to be differences also in the slopes of the CMF vs. eccentricity functions, the variability in the data as well as the problems inherent in estimating CMFs near the fovea make it difficult to conclude that there is a difference in the relative CMF of the various cortical levels between 0.75 and 20 eccentricity. It is well known, however, that extensive reciprocal connections exist among the various cortical areas, and it appears that visual information is progressively integrated at higher levels (cf., Van Essen & Maunsell, 1983). This integrative property of the visual cortex might be expected to average the CMFs of contributing cortical areas and thus reduce the CMF of higher levels. Further, visual receptive field size increases with eccentricity at a greater rate for higher cortical areas (Gattass *et al.*, 1985). These observations are consistent both with the proposition that information is progressively integrated at higher cortical levels and with the present data which indicate a relatively low CMF for the suprathreshold discrimination of complex textures.

Phase-Bandwidth Stimuli. Increasing the phase-bandwidth of two-dimensional, multicomponent Gabor textures, such as the one shown at the upper left in Figure 4, results in a disruption of their spatial structure. As is evident from our analysis of the data of Figure 8 (i.e., the significant bandwidth x eccentricity-size interactions), this disruption is more consistently discriminated at 0.75° than at 20° even when the more peripheral data are magnified by the same factor of four that overcorrected the component-orientation data of Figure 6. This difference is to be expected if positional acuities are required to discriminate the structural differences associated with changes in phase-bandwidth.

Hofmann and Hallett (1993) note that for simple, regular patterns, orientation and phase are effectively local parameters since the changes they induce are easily identifiable with features defined by local differences in luminance. If such features are mediating discrimination, they should scale as luminance or contrast and hence be equatable in the center and periphery. However, in more complex textures such as those used in the present study, the size of the

luminance features may be a limiting factor in discrimination. Changes in phase-bandwidth tend to result in local feature changes that are on a smaller scale than those associated with changing the number of oriented components in a texture. Since spatial features are known to be more difficult to discriminate in the periphery, the differences in the CMF for the #OR and phase bandwidth stimuli may simply be due to a relative undersampling of the present textures in the peripheral visual field (cf., Hess & Pointer, 1987).

It has been suggested (Hofmann & Hallett, 1993; Klein & Tyler, 1986) that textures whose components differ in phase only may be more difficult to discriminate than textures whose components differ in orientation. While both the numbers-of-orientation and phase-bandwidth stimuli of the present study were matched for mean luminance, the effects of visual system nonlinearities, as discussed for example by Bennett and Banks (1991), could result in contrast differences between the standard and comparison images. However, the phase-bandwidth textures were in no case mirror images of each other and so, such nonlinearities cannot explain differences in the discrimination of the two types of stimuli used here.

The largest CMF we were able to test here is below those predicted by the discrimination data described above, and so we cannot conclude that data like those of Figure 8 would not be adequately corrected by the same CMFs used to successfully correct data obtained from other positional tasks. The differences in the CMFs indicated by the data of Figures 6 and 8 do suggest, however, that the low CMF associated with the present suprathreshold texture discrimination (Fig. 6) is not shared by a suprathreshold task presumably dependent on positional cues (Fig. 8). Since this is true of the present stimuli, which are complex textures, it may also be true of phase discriminations in real-world images (Burton & Moorhead, 1981; Oppenheim & Lim, 1981).

Relevance to Simple Models of Texture Segregation

Early theories of texture segregation (e.g., Beck, 1982; Julesz, 1981) considered the effects of various properties (i.e., orientation, closure, terminations, statistical order) of individual texture elements. Some recent models (e.g., Bergen & Landy, 1991; Clark & Bovik, 1989; Graham, Beck & Sutter, 1992; Turner, 1986) have attempted to account for the visual segregation of certain simple textures using local feature analyzers in the form of elementary functions (including Gabor functions) presumed to characterize visual receptive fields. Texture discrimination, however, is more than just texture segregation, and real textures are more complex than those to which models are typically applied. We have generated textures that are complex but nevertheless quantifiable in terms of their Gabor components. They may, therefore, be particularly suitable for testing models of texture discrimination.

As an example of how the present data might be used to assess current texture segregation theories, consider the models of Bergen and Landy (1991) and Graham *et al.* (1992). These models incorporate component channels with a total of only 3-4 different orientations. The most salient feature of the data of Figure 6 is that the number of orientations at which

discrimination asymptotes (i.e., the critical #ORs) is between 5 and 7. Thus, the present results indicate that only a few additional channels would be necessary to adequately model the discrimination of more complex, full gray-scale textures. The critical #ORs estimated here are also consistent with threshold data, which suggest that there are 5-8 orientation channels with bandwidths of 15-30 deg (Dannemiller & Ver Hoeve, 1990; Daugman, 1984; Phillips & Wilson, 1984).

Although it is unlikely that the models can predict the specific perception associated with a stimulus composed of many sinusoidal components, the estimated bandwidth of the presumed underlying mechanisms might lead to a prediction about the global perception of such a stimulus. This estimate might then be inconsistent with the actual perceptual response when the component spatial frequencies and orientations are separated by more than that bandwidth. Such perceived changes are emergent properties of a particular combination of components in the sense that they cannot necessarily be predicted by the presumed response to the individual components. It is not clear whether emergent percepts are related to the overall pattern of activity in the presumed set of mechanisms. However, the emergent percepts become more meaningful if it can be shown that they change in a predictable way with known changes in mechanism properties such as occur, for instance, across the visual field.

As noted above, the textures used in the present experiments were constructed from spectral components whose form is similar to the filters used in some models of texture segregation. For example, the model proposed by Sutter et al., (1989) uses Gabor filters of various orientations and spatial frequencies. These filters correspond quite well to the components of our textures. We therefore attempted to apply the Sutter, Beck, and Graham (SBG) model to the data obtained from rating the similarity of multicomponent textures. In doing this, we assumed that the degree to which a texture pair would segregate perceptually would be inversely related to the pair's rated similarity (i.e., similar pairs would segregate less strongly than dissimilar pairs).

Our implementation of the SBG model used sixteen Gabor filters: four orientations (0, 45, 90, and 135 deg) at each of four spatial frequencies (2, 4, 8, and 16 cycles per image (cpi)). Shown in Figure 9 are examples of the filters that corresponded to each of the four spatial frequencies at a single orientation. Examples of a 2 cpi filter at two orientations differing by 90 degrees are shown in Figure 10. Predictions of similarity ratings for a pair of textures were derived as follows:

(1) The original 256 x 256 texture images were decimated to 128 x 128 arrays, and the 8-bit gray-scale was transformed to the range -128 to 128.

(2) Each of the 16 filters was convolved with a texture array, resulting in 16 convolution arrays for each texture array. The convolution algorithm padded the texture array with zeros out to the size of the resulting convolution array.

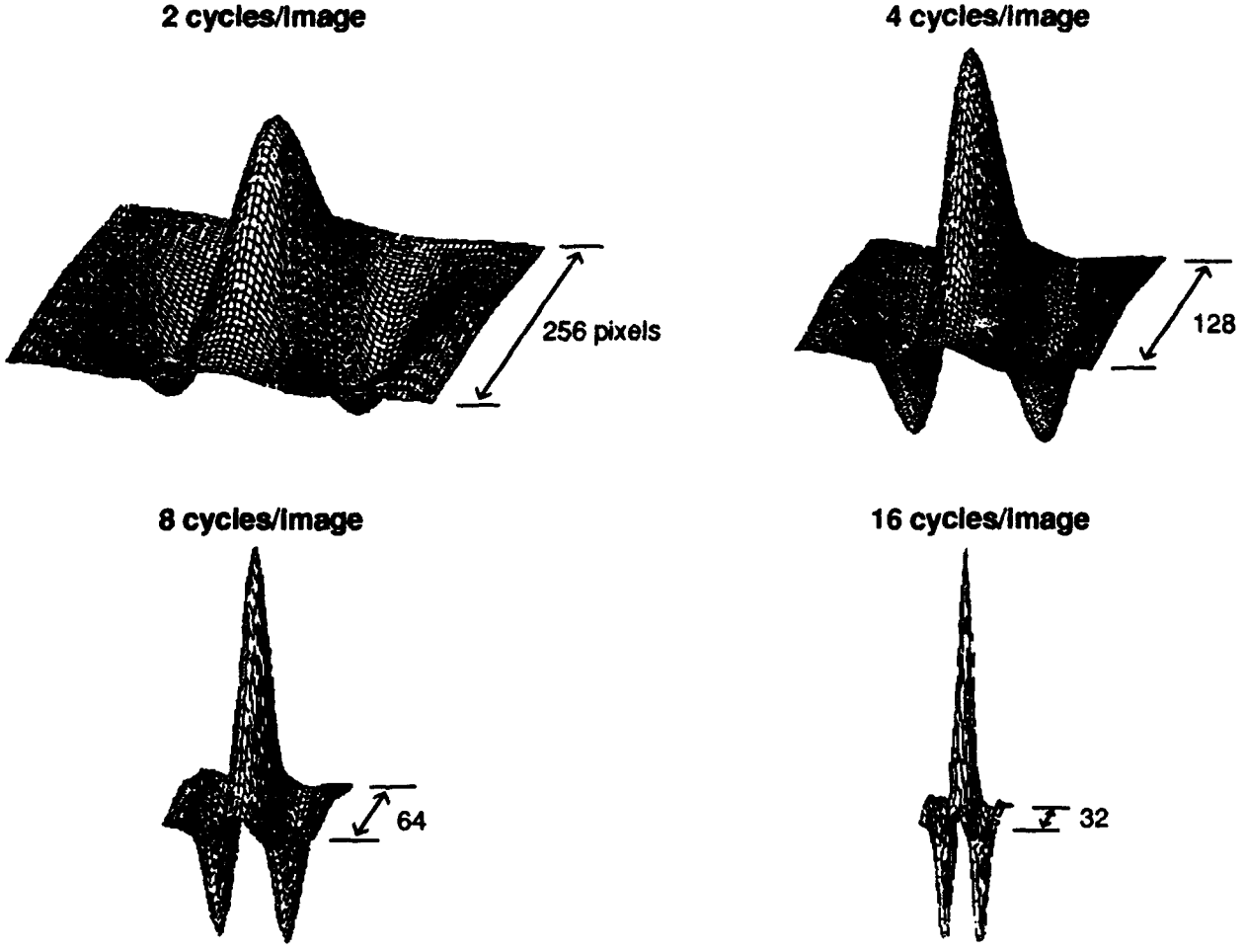

Figure 9

Examples of the Spatial Filters Used to Analyze the Texture Stimuli

The textures were 256x256 pixels and so the filters correspond to spatial frequencies of: 2 cycles per image (cpi), 4 cpi, 8 cpi, and 16 cpi.

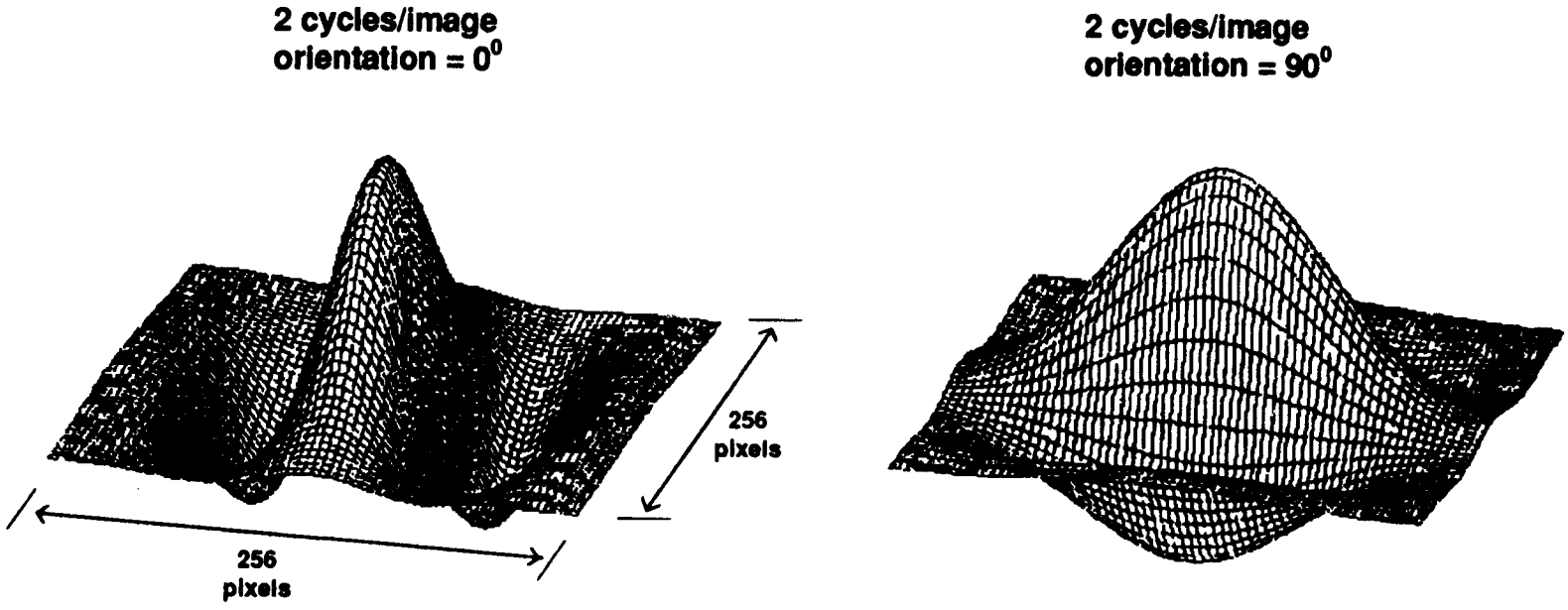

Figure 10
Examples of Spatial Filters of the Same Spatial Frequency (2cpi)
but Differing in Orientation by 90 Degrees

(3) The standard deviation of each convolution array was computed. In the SBG model, this standard deviation is taken to be the spatially pooled response of a particular filter to a stimulus.

(4) In a comparison of two stimulus textures (one of them always a 64-component standard), the difference in pooled response between comparison and standard was computed separately for each of the sixteen filters.

(5) Each of these sixteen difference scores was multiplied by a value representing the sensitivity of the observer to the particular frequency and orientation of the filter. These relative sensitivity values were obtained by interpolation from the same contrast-sensitivity function used by Sutter et al. (1989).

(6) Finally, the corrected filter output differences were squared and summed. This yielded a value which was hypothesized to be proportional to the perceived difference between textures. Thus, larger values should correspond to smaller observed similarity ratings.

The correspondence between predicted difference and observed similarity was found to be poor. In an effort to determine the source of the discrepancies between the model and the data, we applied the model to a variety of simpler stimuli, many composed of only one or two components. The results of these tests highlight some properties of the SBG model which suggest that the model may not be applicable to multicomponent textures.

The texture segregation models mentioned above have been successful in predicting the perceptual segregation of particular, widely used, classes of textures. As noted above, the textures used in the present experiments were constructed from spectral components which might be expected to stimulate the mechanisms postulated in these models. However, the extent to which the presence of a spectral component in the stimulus leads to a corresponding output in the model depends upon the figure of merit used in computing model output. For example, in the simple model of SBG referred to earlier, the output of a filter tuned to a particular spatial frequency and orientation is determined by convolving the filter over the stimulus image and then computing the standard deviation of the elements of the convolution. This method of computing filter output has the property that stimulus components outside the bandwidth of the filter will alter the output value. For example, when we used an exact duplicate of a 16 cpi/ 0-deg filter as a simple input stimulus, the resulting filter output was large, as expected, since stimulus and filter were a perfect match. But when we added a second component at 2 cpi and 90-deg orientation to the input stimulus, filter output was markedly reduced. Thus, the SBG method of computing filter output results in a response measure that is markedly affected by the presence of distant spectral components. For purposes of comparison, we used the same filter and the same two stimuli with a different method of computing filter output, namely, a simple element-by-element multiplication of the filter and stimulus at a single (0 deg) phase. The result of this operation was virtually unaffected by the addition of the 2 cpi/90-deg component. Moreover, although the output computation used by SBG is phase-invariant for a single-component image, when we examined the response of a single filter to images composed of two

components (2 and 16 cpi, 0 orientation), the output of the filter changed with the relative phase of the two components.

The sensitivity to relative phase and to components outside the filter bandwidth described above may be advantageous in some situations, but these properties make the task of applying the model to our multicomponent textures problematic. For example, we must generate predictions about rated similarity between textures that have different (randomized) phase compositions. If the responses to the SBG filters are largely determined by the particular relative phases between components in an image, then they will not reflect the variables that control the responses of our observers (e.g., number of orientations). We ran the SBG model on two of our four standard 64-component images as well as some of the comparison images. Observers see the two standard images as very similar, but the SBG model produces a difference value much greater than the difference between the standards and some comparisons that get very low similarity ratings. We conclude, therefore, that the SBG model does not adequately predict the rated similarity of multicomponent Gabor textures of the form used in the present study. It is not obvious how the SBG model, or any other existing model of texture discrimination can be modified to predict the discrimination of arbitrary texture stimuli. One possibility, however, is to replace the convolution operation with a more general summation operation that better reflects the spatial resolution and two-dimensional spatial frequency characteristics of known visual receptive fields.

REFERENCES

Badcock, D.R. (1984). Spatial phase or luminance profile discrimination? *Vision Research, **24**,* 613-623.

Beck, J. (1966). Effect of orientation and of shape similarity on perceptual grouping. *Perception & Psychophysics, **1**,* 300-302.

Beck, J. (1982). Textural segmentation. In Beck, J. (Ed.), *Organization and representation in perception,* pp. 285-317. Hillsdale, NJ: Lawrence Erlbaum.

Bennett, P.J., & Banks, M.S. (1991). The effects of contrast, spatial scale, and orientation on foveal and peripheral phase discrimination. *Vision Research, **31**,* 1759-1786.

Bergen, J.R., & Landy, M.S. (1991). Computational modeling of visual texture segregation. In Landy, M.S., & Movshon, J.A. (Eds), *Computational models of visual processing,* pp. 253-271. Cambridge: MIT Press.

Braddick, O., Campbell, F.W., & Atkinson, J. (1978). Channels in vision: Basic aspects. In *Handbook of sensory physiology,* **Vol. 8**, 3-38.

Burton, G.J., & Moorhead, I.R. (1981). Visual form perception and the spatial phase transfer function. *Journal of the Optical Society of America, **71**,* 1056-1063.

Caelli, T. (1982). On discriminating visual textures and images. *Perception & Psychophysics, **31**,* 149-159.

Caelli, T., & Bevan, P. (1983). Probing the spatial frequency spectrum for orientation sensitivity in stochastic textures. *Vision Research, **23**,* 39-45.

Campbell, F.W., & Robson, J.G. (1968). Application of Fourier analysis to the visibility of gratings. *Journal of Physiology* (Lond.), ***197***, 551-566.

Cannon, M.W., & Fullenkamp, S.C. (1988). Perceived contrast and stimulus size: Experiment and simulation. *Vision Research, **28**,* 695-709.

Carpenter, R.H.S., & Blakemore, C. (1973). Interactions between orientations in human vision. *Experimental Brain Research, **18**,* 287-303.

Clark, M., & Bovik, A.C. (1989). Experiments in segmenting texton patterns using localized spatial filters. *Pattern Recognition, **22**,* 707-717.

Daniel, P.M., & Whitteridge, D. (1961). The representation of the visual field in the cerebral cortex in monkeys. *Journal of Physiology (London), **159**,* 203-221.

Dannemiller, J.L., & Ver Hoeve, J.N. (1990). Two-dimensional approach to psychophysical orientation tuning. *Journal of the Optical Society of America A, **7**,* 141-151.

Daugman, J.G. (1980). Two-dimensional spectral analysis of cortical receptive field profiles. *Vision Research, 20,* 847-856.

Daugman, J.G. (1984). Spatial visual channels in the Fourier plane. *Vision Research, 24,* 891-910.

Dow, B.M., Snyder, A.Z., Vautin, R.G., & Bauer, R. (1981). Magnification factor and receptive field size in foveal striate cortex of the monkey. *Experimental Brain Research, 44,* 213-228.

Enroth-Cugell, C., & Robson, J.G. (1966). The contrast sensitivity of retinal ganglion cells of the cat. *Journal of Physiology* (Lond.), *187,* 517-552.

Field, D.J. (1987). Relations between the statistics of natural images and the response properties of cortical cells. *Journal of the Optical Society of America A, 4,* 2379-2394.

Fogel, I., & Sagi, D. (1989). Gabor filters as texture discriminator. *Biological Cybernetics, 61,* 103-113.

Gattass, R., Sousa, A.P.B., & Covey, E. (1985). Cortical visual areas of the macaque: Possible substrates for pattern recognition mechanisms. In Chagas, C., Gattass, R. & Gross, C. (Eds.), *Pattern recognition mechanisms,* pp. 1-20. Berlin: Springer-Verlag.

Georgeson, M.A., & Harris, M.G. (1984). Spatial selectivity of contrast adaptation: models and data. *Vision Research, 24,* 729-741.

Geri, G.A., & Lyon, D.R. (1991). The spatial extent of shape adaptation in the central and peripheral visual fields. In B. Blum (Ed.) *Channels in the visual nervous system: Neurophysiology, psychophysics and models,* pp. 87-108. London: Freund.

Geri, G.A., Lyon, D.R., & Zeevi, Y.Y. (1989). Discrimination of multicomponent Gabor textures in the central and peripheral visual field. *Investigative Ophthalmology & Visual Science (Suppl.), 30,* 452.

Geri, G.A., Lyon, D.R., & Zeevi, Y.Y. (1990). Phase discrimination of multicomponent Gabor textures in the central and peripheral visual field. *Investigative Ophthalmology & Visual Science (Suppl.), 31,* 104.

Geri, G.A., Zeevi, Y.Y., & Porat, M. (1990). Efficient image generation using localized frequency components matched to human vision. (AFHRL-TR-90-25, AD A224 903). Williams Air Force Base, AZ: Operations Training Division, Air Force Human Resources Laboratory.

Graham, N. (1989). *Visual pattern analyzers.* New York: Oxford University Press.

Graham, N., Beck, J., & Sutter, A. (1992). Nonlinear processes in spatial-frequency channel models of perceived texture segregation: Effects of sign and amount of contrast. *Vision Research, 32,* 719-743.

Graham, N., & Nachmias, J. (1971). Detection of grating patterns containing two spatial frequencies: A comparison of single-channel and multiple-channel models. *Vision Research, 11*, 251-259.

Hess, R.F., & Pointer, J.S. (1987). Evidence for spatially local computations underlying discrimination of periodic patterns in fovea and periphery. *Vision Research, 27*, 1343-1360.

Hofmann, M.I., & Hallett, P.E. (1993). Texture segregation based on two-dimensional relative phase differences in composite sine-wave grating patterns. *Vision Research, 33*, 221-234.

Hubel, D.H., & Wiesel, T.N. (1962). Receptive fields, binocular interaction and functional architecture in the cat's visual cortex. *Journal of Physiology* (Lond.), *160*, 106-154.

Hubel, D.H., & Wiesel, T.N. (1968). Receptive fields and functional architecture of monkey striate cortex. *Journal of Physiology* (Lond.), *195*, 215-243.

Hubel, D.H., & Wiesel, T.N. (1974). Uniformity of monkey striate cortex: A parallel relationship between field size, scatter, and magnification factor. *Journal of Comparative Neurology, 158*, 295-306.

Johnston, A. (1987). Spatial scaling of central and peripheral contrast-sensitivity functions. *Journal of the Optical Society of America A, 4*, 1583-1593.

Jones, J.P., & Palmer, L.A. (1987). An evaluation of the two-dimensional Gabor filter model of simple receptive fields in cat striate cortex. *Journal of Neurophysiology, 58*, 1233-1258.

Julesz, B. (1981). Textons, the elements of texture perception, and their interactions. *Nature, 290*, 91-97.

Klein, S.A., & Levi, D.M. (1987). Position sense of the peripheral retina. *Journal of the Optical Society of America A, 4*, 1543-1553.

Klein, S.A., & Tyler, C.W. (1986). Phase discrimination of compound gratings: Generalized autocorrelation analysis. *Journal of the Optical Society of America A, 3*, 868-879.

Kronauer, R.E., Daugman, J.G., & Zeevi, Y.Y. (1982). Degree of disorder perceived in images with punctate spectra. *Journal of the Optical Society of America, 72*, 1798.

Lamme, V.A.F., Van Dijk, B.W., & Spekreijse, H. (1992). Texture segregation is processed by primary visual cortex in man and monkey. Evidence from VEP experiments. *Vision Research, 32*, 797-807.

Lawton, T.B. (1984). The effect of phase structures on spatial phase discrimination. *Vision Research, 24*, 139-148.

Levi, D.M., & Klein, S.A. (1985). Vernier acuity, crowding and amblyopia. *Vision Research, 25,* 979-991.

Levi, D.M., Klein, S.A., & Aitsebaomo, A.P. (1985). Vernier acuity, crowding and cortical magnification. *Vision Research, 25,* 963-977.

Malik, J., & Perona, P. (1990). Preattentive texture discrimination with early vision mechanisms. *Journal of the Optical Society of America A, 7,* 923-932.

Nothdurft, H.C. (1985). Orientation sensitivity and texture segmentation in patterns with different line orientations. *Vision Research, 25,* 551-560.

Oppenheim, A.V., & Lim, J.S. (1981). The importance of phase in signals. *Proceedings of the IEEE, 69,* 529-541.

Paradiso, M.A., & Carney, T. (1988). Orientation discrimination as a function of stimulus eccentricity and size: Nasal/temporal retinal asymmetry. *Vision Research, 28,* 867-874.

Phillips, G.C., & Wilson, H.R. (1984). Orientation bandwidths of spatial mechanisms measured by masking. *Journal of the Optical Society of America A, 1,* 226-232.

Porat, M., & Zeevi, Y.Y. (1988). The generalized Gabor scheme of image representation in biological and machine vision. *IEEE Transactions on Pattern Analysis and Machine Intelligence, 10,* 452-468.

Porat, M., & Zeevi, Y.Y. (1989). Localized texture processing in vision: Analysis and synthesis in the Gaborian space. *IEEE Transactions on Biomedical Engineering, 36,* 115-129.

Quick, R.F. (1974). A vector-magnitude model of contrast detection. *Kybernetik, 16,* 65-67.

Raninen, A., & Rovamo, J. (1986). Perimetry of critical flicker frequency in human rod and cone vision. *Vision Research, 26,* 1249-1255.

Richards, W., & Polit, A. (1974). Texture matching. *Kybernetik, 16,* 155-162.

Rovamo, J., & Virsu, V. (1979). An estimation and application of the human cortical magnification factor. *Experimental Brain Research, 37,* 495-510.

Rovamo, J., Virsu, V., & Näsänen, R. (1978). Cortical magnification factor predicts the photopic contrast sensitivity of peripheral vision. *Nature, 271,* 54-56.

Schachter, B. (1980). Long crested wave models. *Computer Graphics and Image Processing, 12,* 187-201.

Schachter, B. (1983). *Computer image generation*, pp. 156-161. New York: Wiley-Interscience.

Scobey, R.P. (1982). Human vsual orientation discrimination. *Journal of Neurophysiology, 48,* 18-26.

Snyder, A.W. (1982). Hyperacuity and interpolation by the visual pathways. *Vision Research, 22,* 1219-1220.

Sutter, A., Beck, J., & Graham N. (1989). Contrast and spatial variables in texture segregation: Testing a simple spatial-frequency channels model. *Perception & Psychophysics,* **46**, 312-332.

Talbot, S.A., & Marshall, W.H. (1941). Physiological studies on neural mechanisms of visual localization and discrimination. *American Journal of Ophthalmology, 24,* 1255-1264.

Thomas, J.P. (1985). Detection and identification: How are they related. *Journal of the Optical Society of America A, 2,* 1457-1467.

Turner, M.R. (1986). Texture discrimination by Gabor functions. *Biological Cybernetics, 55,* 71-82.

Van Essen, D.C., & Maunsell, H.R. (1983). Hierarchical organization and functional streams in the visual cortex. *Trends in Neuroscience, 6,* 370-375.

Van Essen, D.C., Newsome, W.T., & Maunsell, H.R. (1984). The visual field representation in striate cortex of the macaque monkey: Asymmetries, anisotropies, and individual variability. *Vision Research, 24,* 429-448.

Virsu, V., Näsänen, R., & Osmoviita, K. (1987). Cortical magnification and peripheral vision. *Journal of the Optical Society of America A, 4,* 1568-1578.

Watson, A.B. (1982). Summation of grating patches indicates many types of detector at one retinal location. *Vision Research, 22,* 17-26.

Watson, A.B. (1983). Detection and recognition of simple spatial forms. In *Physical and biological processing of images* (O.J. Braddick & A.C. Sleigh, Eds.). New York: Springer-Verlag.

Wilson, H.R., & Bergen, J. (1979). A four-mechanism model for threshold spatial vision. *Vision Research,* **19**, 19-32.

Zeevi, Y.Y., & Gertner, I. (1992). The finite Zak transform: An efficient tool for image representation and analysis. *Journal of Visual Communication and Image Representation, 3,* 13-23.

Zeevi, Y.Y., Porat, M., & Geri, G.A. (1990). Computer image generation for flight simulators: The Gabor approach. *The Visual Computer, 6,* 93-105.